

# **Displacement and velocity measurements using homodyne interferometry**

DENIS MOUNIER

# Table des matières

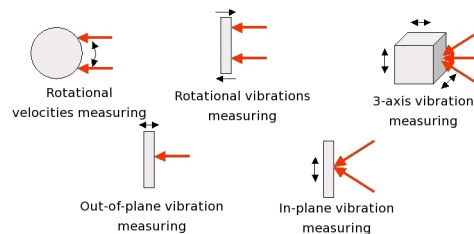
<b>I. Course</b>	<b>3</b>
1. Principles used in displacement and velocity measurements.....	<b>3</b>
1.1. Frequency modulation of a light wave using the Doppler effect.....	<b>3</b>
1.2. Detection of the Doppler shift using a Fabry-Perot interferometer.....	<b>6</b>
1.3. Relation between phase modulation and displacement of the target.....	<b>8</b>
1.4. Two-beam interferometry.....	<b>8</b>
2. Homodyne interferometry.....	<b>15</b>
2.1. Definition.....	<b>15</b>
2.2. Description of a homodyne Michelson interferometer.....	<b>15</b>
2.3. Displacement measuring using fringe counting.....	<b>18</b>
2.4. Demodulation of a homodyne signal.....	<b>20</b>
2.5. Measuring ultrasonic vibrations.....	<b>21</b>
2.6. Advantages and drawbacks of the homodyne interferometer.....	<b>37</b>
<b>II. Case study</b>	<b>38</b>
1. Measurements of ultrasonic vibrations up to 1GHz.....	<b>38</b>
<b>III. Exercises</b>	<b>42</b>
1. Questions.....	<b>42</b>
2. Exercise.....	<b>43</b>
<b>Solution des exercices</b>	<b>44</b>
<b>Bibliographie</b>	<b>45</b>
<b>Webographie</b>	<b>46</b>

# I.Course

## 1. Principles used in displacement and velocity measurements

This chapter focuses on optical measurements of displacements or velocities. However, only the measuring instruments that include an interferometer will be considered: *laser vibrometer*, *Doppler laser velocimetry* devices, *laser trackers*, *laser gyrometers*.

**Laser vibrometers** are instruments used to measure vibrations. They can measure displacements or instantaneous velocities on a remote localised target and, thanks to its laser beam, without any contact. The bandwidth of the laser vibrometers that can be purchased vary from some Hertz to 1 GHz. The smallest amplitudes measurable can usually reach  $10^{-9}$  m. Using several laser beams, three dimensional vibration measurements and rotational measurements are available



Contrary to laser vibrometers, which can measure displacements usually limited to several  $\mu\text{m}$ , occasionally some mm, laser trackers are used for the three dimensional metrology of large items. The measuring ranges go from a few centimetres to several dozens of meters.

This chapter focuses only on interferometry-based devices. The devices using "self-mixing", which provide displacement and velocity measurements as well, will not be considered. Similarly, displacement measurement instruments based on measuring a light pulse time-of-flight or on phase-shifting a modulated light will not be tackled.

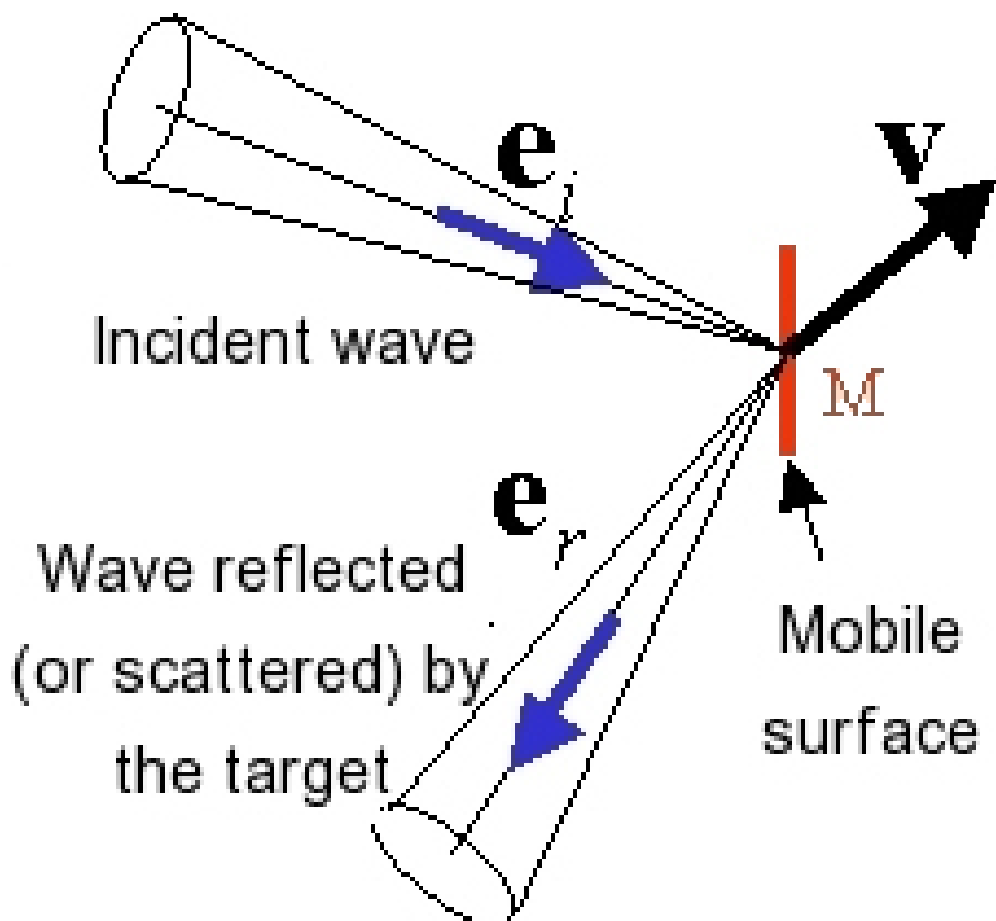
The first part of this course will examine the optical velocity measurement principle of a moving target. Then, a few examples of interferometry assemblies will be given. A large part will focus on homodyne laser vibrometry and will be the perfect opportunity to introduce the notions of detection limit and signal-to-noise ratio. The part on heterodyne interferometry can be linked with three dimensional vibrometry techniques, with "in-plane" velocimetry, Doppler laser anemometry and rotational velocimetry, which all use heterodyne interferometry.

The case study will underline the performances of a homodyne vibrometer measuring ultrasound up to 1 GHz.

### 1.1. Frequency modulation of a light wave using the Doppler effect

We consider a quasi-monochromatic light wave with a centre frequency  $\nu_0$  and a linewidth  $\delta\nu$ , small compared to its center frequency  $\nu_0$ . Most of the laser sources are quasi-monochromatic. We suppose that the light wave focuses on a target point M located on a mobile scattering surface, with a velocity  $\mathbf{v}$  in the referential frame linked to the laser source. The incident wave on the target is characterised by a wave vector  $\vec{k}_i$  and the scattered wave is

characterised by a wave vector  $\vec{k}_i$ . The unit vectors associated to the incidence and observation directions are respectively :

$$\vec{e}_i = \frac{\vec{k}_i}{\|\vec{k}_i\|} \quad \vec{e}_r = \frac{\vec{k}_r}{\|\vec{k}_r\|}$$


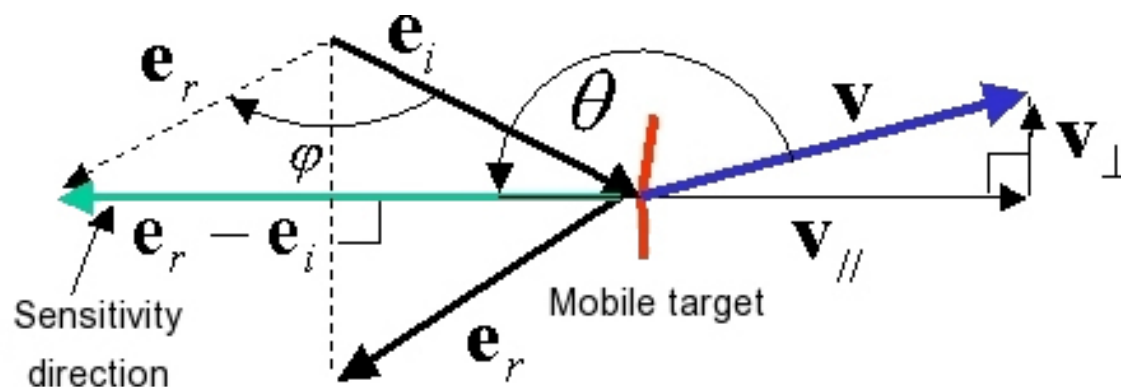
### Fondamental

The light wave *scattered* or *reflected* by the moving target undergoes an instant frequency phase shift  $\delta\nu_D(t)$ , known as **Doppler shift**, and equal to:

$$\delta\nu_D = \frac{\vec{v} \cdot (\vec{e}_r - \vec{e}_i)}{\lambda}$$

The instantaneous frequency of the reflected wave  $\nu(t) = \nu_0 + \delta\nu_D(t)$  is **modulated in frequency** by the target's movement.

On the basis of Equation 1, we can see that the Doppler shift is the highest if the direction of the velocity  $\vec{v}$  is collinear to the sensitivity vector  $\vec{e}_r - \vec{e}_i$ .



Consequently, measuring the three components of velocity (three-dimensional measurements) requires three laser beams, with non-collinear sensitivity vectors.

With the angles  $\varphi$  and  $\theta$  determined by figure 3, equation 1 can be written as:

$$\delta v_{D(i)} = \frac{2v(t)}{\lambda} \sin\left(\frac{\varphi}{2}\right) \cos \theta$$

Doppler laser anemometry (DLA) and Doppler laser velocimetry (DLV) techniques take advantage of the Doppler shift to measure velocities of airborne particles moved by a gas or a liquid.

### Remarque

Knowing that the wave vector and the beat of a wave are respectively:  $k = \frac{2\pi}{\lambda}$  and  $\omega = 2\pi\nu$ , we can write the Doppler shift as:  $\delta\omega_D = \vec{v} \cdot (\vec{k}_r - \vec{k}_i)$ .

### Remarque

We need to point out that the formula of the Doppler shift given by equation 1 is actually an approximation. However, the corrective term, proportional to  $\frac{v^2}{c^2}$ , is insignificant for velocities up to a tenth of the light velocity. The relative error in the approximate formula is inferior to  $10^{-4}$  for velocities up to a 1000 km/s !

### Complément

The Doppler shift phenomenon is also known in acoustics. It shows when a sound source is in motion in comparison to observers. The observers feel a higher sound frequency when the source is moving toward them and a lower one when it is moving away. The same phenomenon happens when the sound source is immobile and the observers are moving toward it. The Doppler shift is determined by the relative motion between the source and the observers.

To determine the formula of a light wave's Doppler shift, we shall define a first referential frame  $\mathfrak{R}_0$  in which the primary light source is fixed, and a second one  $\mathfrak{R}$  led by the target which acts as a mobile secondary light source. In the referential frame  $\mathfrak{R}_0$ , the source emits a frequency wave  $\nu_0 = c/\lambda$  in the direction of the unit vector  $\vec{e}_i$ . The target is moving at a velocity  $\vec{v} = \vec{v}(\mathfrak{R}/\mathfrak{R}_0)$ . An immobile observer located in  $\mathfrak{R}$  can see the incident wave on the

target at a frequency equal to  $\nu_1 = \gamma\nu_0\left(1 - \frac{\vec{v} \cdot \vec{e}_i}{c}\right)$  with  $\gamma = \frac{1}{\sqrt{1 - \frac{v^2}{c^2}}}$ . For readers acquainted with the language of restricted relativity, the frequency transformation formula can be directly

found using the Lorentz transformation on the four-wave vector  $(\omega, \vec{k})$ . For an immobile observer located in  $\mathfrak{R}$ , the incident and scattered waves have the same frequency  $\nu_1$  because we assume that the photon diffusion process is perfectly flexible (when it comes to the Rayleigh scattering). Reciprocally, we can write a similar relation for the scattered light:

$$\nu_2 = \gamma \nu_1 \left(1 - \frac{\vec{v} \cdot \vec{e}_r}{c}\right),$$

in which  $\nu_2$  represents the frequency of the wave which is scattered in the direction of the unit vector  $\vec{e}_r$  and seen by an immobile observer located in the referential frame  $\mathfrak{R}_0$ . The reciprocity between the absorption and emission processes is outstanding and

$$\nu_2 = \nu_0 \left( \frac{1 - \frac{\vec{v} \cdot \vec{e}_i}{c}}{1 - \frac{\vec{v} \cdot \vec{e}_r}{c}} \right)$$

leads to the relation

A development limited to a single variable in  $v/c$  gives the approximate relation

$$\nu_2 = \nu_0 \left[ 1 + \frac{\vec{v} \cdot (\vec{e}_r - \vec{e}_i)}{c} \right]$$

and the Doppler shift  $\delta\nu_D = \nu_2 - \nu_0 = \frac{\vec{v} \cdot (\vec{e}_r - \vec{e}_i)}{\lambda}$ .

## 1.2. Detection of the Doppler shift using a Fabry-Perot interferometer

When velocities are high enough, the Doppler shift  $\delta\nu_D$  can, in theory, be detected by a high resolution spectrometer. This is true in astronomy: the velocities of stars or galaxies are quantified using the Doppler shift of well-identified atomic spectral lines. In this case, since the object is emitting the light that the observers receive, it is necessary to use the formula

$$\delta\nu_D = \frac{\vec{v} \cdot \vec{e}_r}{\lambda},$$

in which  $\vec{e}_r$  is the unit vector of the direction between the object and the observers.

### Exemple

We consider the case of a target moving at a speed of 100 m/s speed and reflecting in a normal incidence a light wave with a wavelength equal to 500 nm. The Doppler shift after reflection is of 400 MHz. Measuring such a shift can theoretically be done with a high resolution spectrometer, such as a Fabry-Perot interferometer. A Fabry-Perot cavity is made of two parallel plain mirrors, separated from each other by a distance  $e$ , and both having a reflectance  $R$ . We assume that the air, with a  $n \approx 1$ , index, fills the space between both mirrors. The Fabry-Perot cavity transmits as a narrow band-pass filter would. For a plain wave with an incidence angle on the mirrors  $i$  and neglecting the mirrors' absorption, the

transmittance of a Fabry-Perot cavity is given by the Airy function:

$$T(\nu) = \frac{1}{1 + M \sin^2(\phi/2)},$$

in which  $M = \frac{4R}{(1-R)^2}$  and  $\phi = \frac{4\pi e \cos i}{c} \nu$ . With a normal incidence ( $i=0$ ), the transmittance changes along a period  $\Delta\nu = c/(2e)$ , which is the *free spectral range* of the cavity. The width of

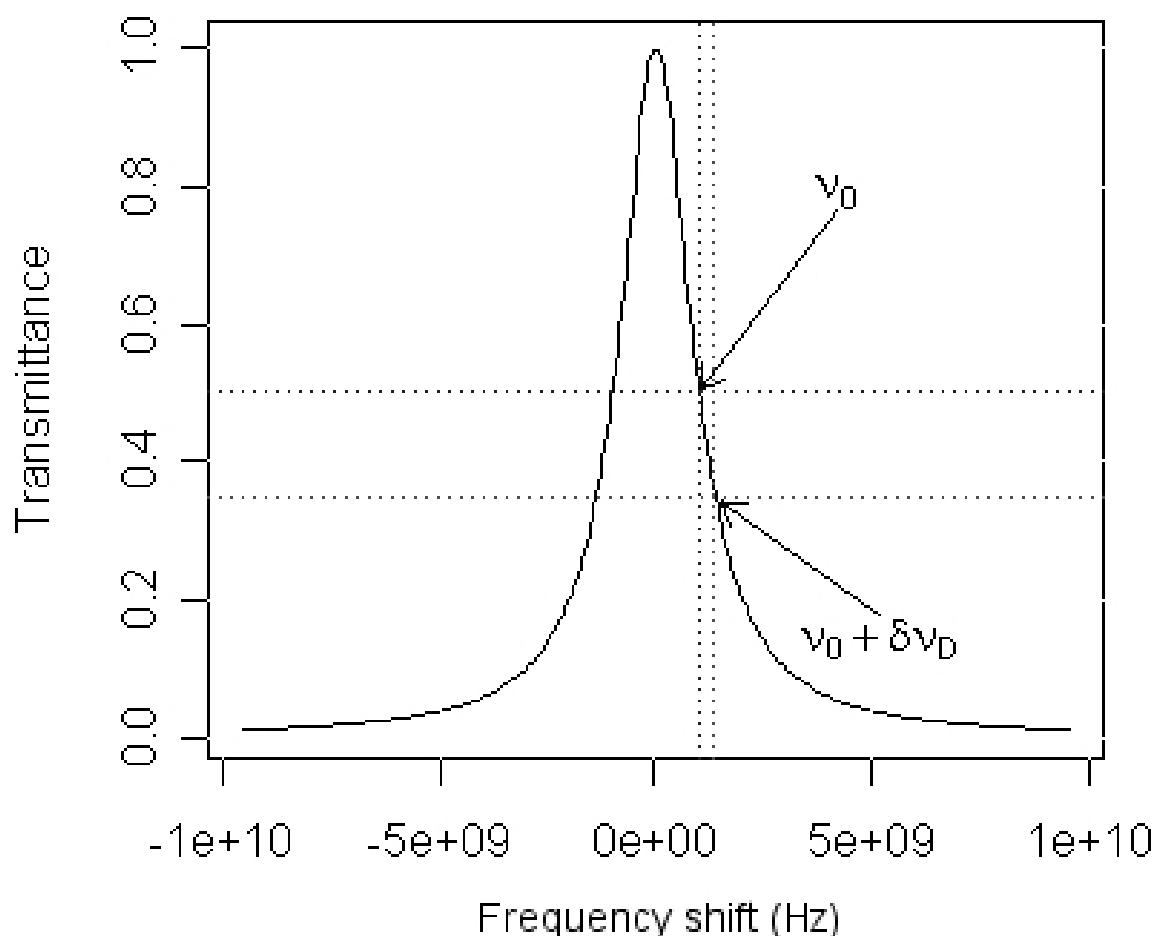
a spectral line located half way of the Fabry-Perot is  $\delta\nu = \Delta\nu/F$  in which  $F = \frac{\pi M^{1/2}}{2}$  represents the *precision* of the Fabry-Perot cavity. The transmission pattern of a Fabry-Perot's spectral line is shown on figure 4 ("Fabry-Perot") depending on the frequency shift, for mirrors having a  $R = 0.9$  reflectance and separated from each other by a distance  $e = 5$  mm. A high precision in the Fabry-Perot spectral lines is responsible for a high sensitivity to frequency shifts. Let's assume that we use a quasi-monochromatic laser source, with a frequency  $\nu_0$  and a line width way inferior to the Fabry-Perot line width:  $\delta\nu_0 \ll \delta\nu$ . In order to reach the highest sensitivity to small frequency variations near  $\nu_0$ , the length of the Fabry-Perot cavity must be locked so that

some 50% of the frequency  $\nu_0$  should be transmitted. The optimal working point of the cavity is reached at an inflexion point and at the peak of the transmittance curve slope. Then, a small variation of an incident wave's frequency results in a significant variation of the power transmitted by the cavity. Figure 4 shows that 50% of the laser line having a frequency  $\nu_0$  is transmitted and that only 35% of the frequency  $\nu_0 + \delta\nu_D$ , changed by a Doppler shift of about 400 MHz, is. The relative change of the transmitted power is of  $7.5 \times 10^{-4} / \text{MHz}$

This corresponds to a sensitivity of:

$$7,5 \times 10^{-4} \times \frac{400 \text{ MHz}}{100 \text{ m/s}} = 3 \times 10^{-3} / (\text{m/s})$$

### Fabry-Perot : R=0.9 and e=5mm



The Doppler shifts are relatively low compared to the frequency of the light wave. To measure them, the laser source must have a single frequency and a line width smaller than  $\delta\nu_D$ . Moreover, the frequency drift of the laser source, during the measuring stage, must be negligible compared to  $\delta\nu_D$ . A single mode laser with a line width inferior to 1 MHz is suitable to measure velocities higher than 0.25 m/s. It is also necessary to slave the length of the cavity in order to maintain a constant and maximal sensitivity. This is why a Fabry-Perot interferometer is not suitable to measure steady velocities or velocities changing too slowly. However, it will work perfectly to detect ultrasonic vibrations with high frequencies, usually between 10 MHz and 100 MHz.

### 1.3. Relation between phase modulation and displacement of the target

A wave light *frequency-modulated* by the velocity of the moving target can also be considered as a *phase-modulated* wave light. Let's consider an elementary time interval  $dt$  which includes a lot of light wave's periods.  $dt \gg 1/\nu_0$  is high compared to the light vibration's period but small compared to the shortest target's vibration period. This latter condition is verified for vibration frequencies up to  $10^{12} \text{ Hz} - 10^{13} \text{ Hz}$ , knowing that a light vibration frequency is usually of  $10^{15} \text{ Hz}$ . During the time interval  $dt$ , the variation of the wave's phase due to the

Doppler shift is:  $d\varphi = 2\pi\delta\nu_D(t)dt$  (by definition, the instantaneous frequency is  $\nu = \frac{1}{2\pi} \frac{d\varphi}{dt}$ ).

During the fixed time interval  $t$ , the phase shift is of  $\Delta\varphi(t) = 2\pi \int_0^t \delta\nu_D(t)dt$ . The amplitude of the light wave can be written  $s_r(r, t) = A_r \cos [2\pi\nu_0 t + \Delta\varphi(t) + \varphi_0]$ , in which

$\Delta\varphi(t) = 2\pi \int_0^t \frac{\vec{v}(t) \cdot (\vec{e}_r - \vec{e}_i)}{\lambda} dt = 2\pi \frac{(\vec{e}_r - \vec{e}_i)}{\lambda} \int_0^t \vec{v}(t') dt' = 2\pi \frac{(\vec{e}_r - \vec{e}_i) \cdot \Delta\vec{r}}{\lambda}$ , and  $\Delta\vec{r}$  represents the displacements between the instants  $t = 0$  and  $t$ .

#### Fondamental

The relation between phase shift and displacement is:

$$\Delta\varphi(t) = \frac{2\pi}{\lambda} (\vec{e}_r - \vec{e}_i) \cdot \Delta\vec{r}$$

#### Remarque

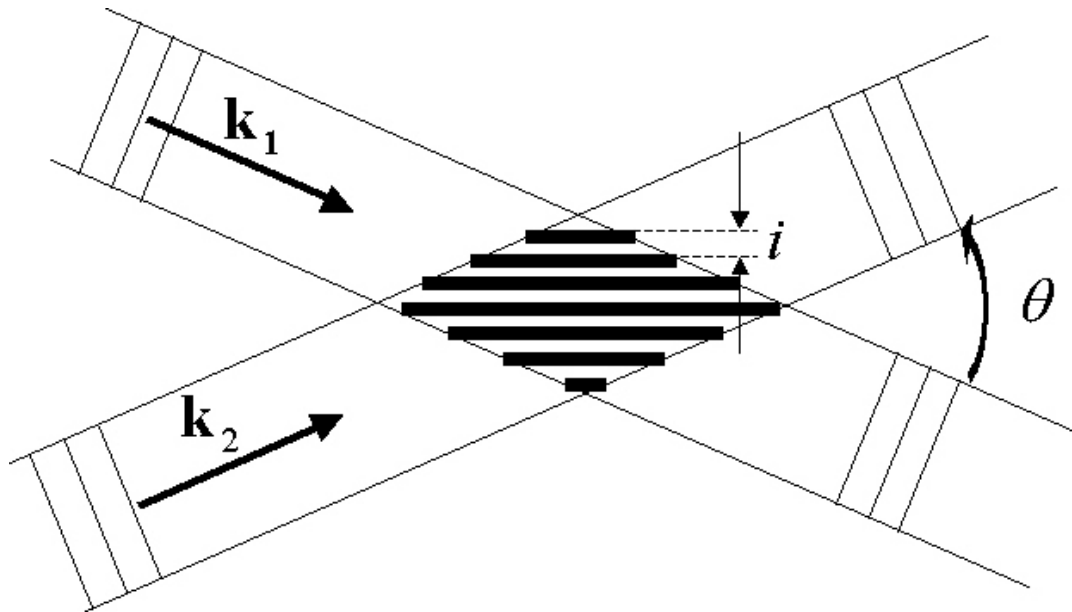
This result presumes that the sensitivity vector  $\vec{e}_r - \vec{e}_i$  does not significantly change during the integration interval. This implies that the target is moving slowly compared to the distances between the laser source's target and the detector. The last relation shows that the phase shift is proportional to the displacement  $\Delta\vec{r}$ .

For practical purposes, measuring the phase shift of a light wave, and thus of an object's displacement, can be done with a two-beam interferometer. One of these two waves, the *reference wave*, has a constant frequency (constant phase) whereas the other one, the *probe wave*, is frequency-modulated (or phase-modulated) by the velocity of the target.

### 1.4. Two-beam interferometry

#### a) Interference between two plain waves

Let's consider two monochromatic collimated light beams, which are coplanar and making an angle  $\theta$ . Both beams being collimated, we will consider them as two monochromatic plane waves.



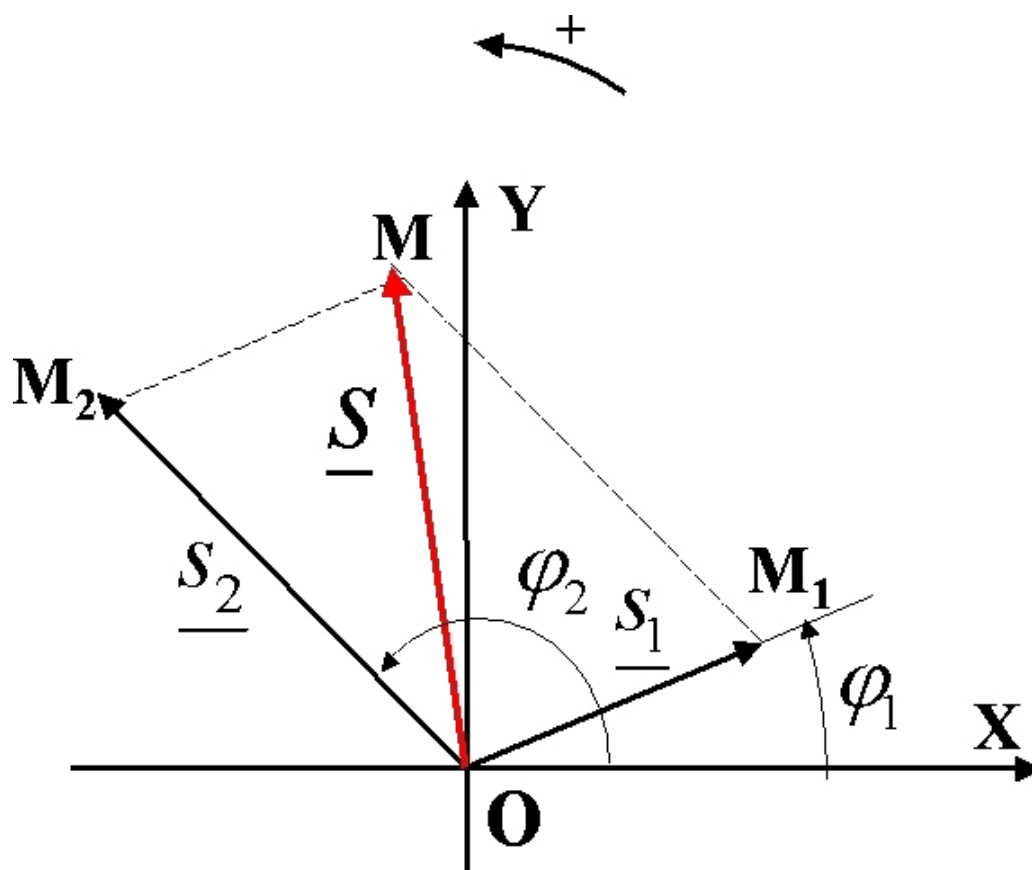
Each wave is defined by the constant frequencies  $\nu_1$  and  $\nu_2$  and by the wave vectors  $\vec{k}_1$  and  $\vec{k}_2$ . Moreover, we assume that the frequencies are almost equal to  $|\nu_1, \nu_2| \ll \nu_1, \nu_2$ .

$$\lambda_1 = \frac{2\pi}{\|\vec{k}_1\|} \quad \lambda_2 = \frac{2\pi}{\|\vec{k}_2\|}$$

The associated wavelengths are  $\frac{2\pi}{\|\vec{k}_1\|}$  and  $\frac{2\pi}{\|\vec{k}_2\|}$ . The actual representations of the wave fields are:  $s_1 = A_1 \cos(2\pi\nu_1 t - \vec{k}_1 \cdot \vec{r} + \varphi_{01})$  and  $s_2 = A_2 \cos(2\pi\nu_2 t - \vec{k}_2 \cdot \vec{r} + \varphi_{02})$ .

These vibrations can be represented by a complex expression:  $s_i = \Re\{A_i \exp[j(2\pi\nu_i t - \vec{k}_i \cdot \vec{r} + \varphi_{0i})]\}$ , with  $i = 1, 2$ , and in which  $\Re$  means "real part".

The complex representation is given by a Fresnel pattern.



The superposition of both wave fields leads to a vector sum of Fresnel vectors  $\vec{OM}_1$  and  $\vec{OM}_2$ .

The argument of the complex amplitude  $s_i$  and  $\varphi_i = 2\pi\nu_i t - \vec{k}_i \cdot \vec{r} + \varphi_{0i}$ . The square module of the vector  $OM$  gives the corresponding light intensity (proportional to the light power density)

$I = s \cdot s^* = I_1 + I_2 + 2\sqrt{I_1 I_2} \cos [\Phi(\vec{r}, t)]$ , in which  $I_1 = A_1^2$ ,  $I_2 = A_2^2$  and

$\Phi(r, t) = 2\pi(\nu_2 - \nu_1)t + (\vec{k}_1 - \vec{k}_2) \cdot \vec{r} + \Phi_0$ . The light intensity in the interference field undergoes a sinusoidal double modulation: a *sinusoidal time modulation* to the frequency  $\nu_2 - \nu_1$  because of the term  $2\pi(\nu_2 - \nu_1) \cdot t$  and a *sinusoidal spatial modulation* according to the *spatial frequency*

vector:  $\frac{\vec{k}_1 - \vec{k}_2}{2\pi}$ , because of the term  $(\vec{k}_1 - \vec{k}_2) \cdot \vec{r}$ . The *period* of the spatial modulation is, by

definition, the *interfringe*:  $i = \frac{2\pi}{\|\vec{k}_1 - \vec{k}_2\|}$ .

It depends on the average wavelength  $\lambda$  of the two waves and of the angle  $\theta$  between both beams:

$$i = \frac{\lambda}{2 \cdot \sin(\frac{\theta}{2})}$$

### Fondamental

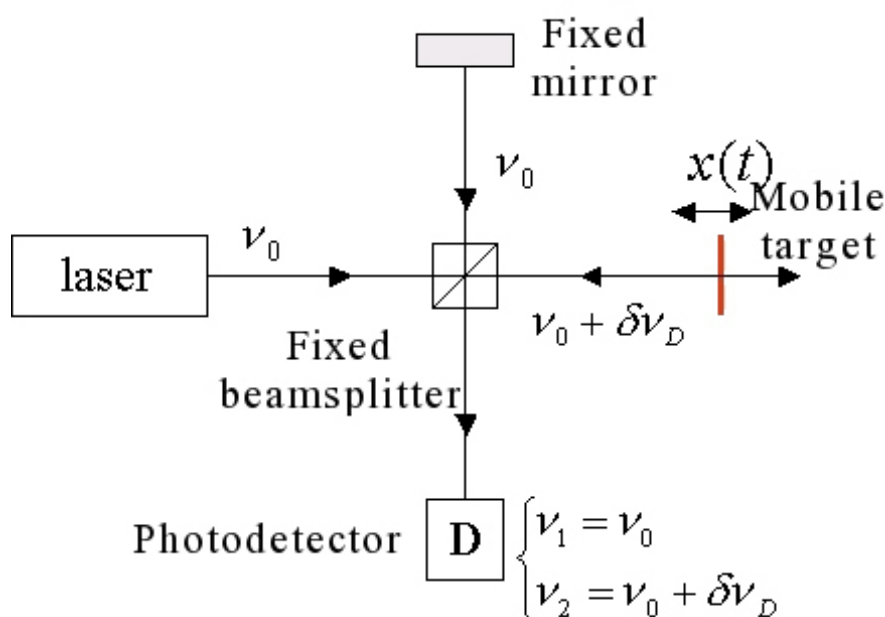
The light intensity of the interference field can be written as  $I = I_0(1 + m \cos \Phi)$ , in

which  $m = \frac{2\sqrt{I_1 I_2}}{I_1 + I_2}$  is the *interference contrast* and  $I_0 = I_1 + I_2$  is the *average intensity inside the interference field*.

## b) Examples of two-beam interferometers

*Exemple*

Let's focus on the Michelson interferometer (Figure 7).

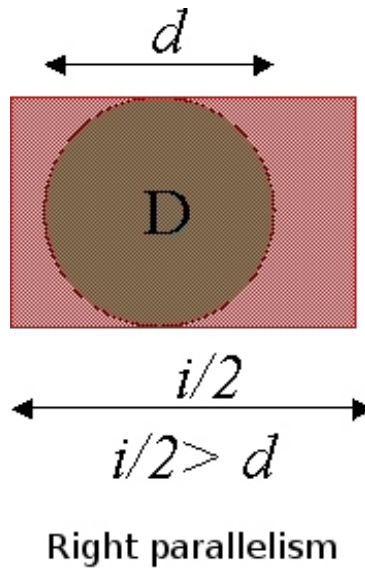


### Michelson interferometer

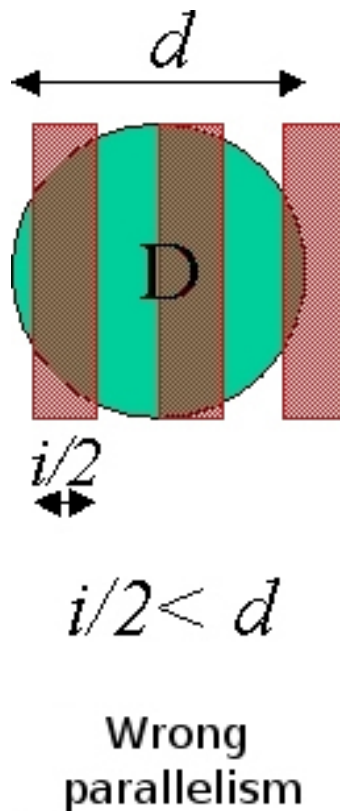
A frequency wave  $\nu_0$  is emitted by a laser as a low-divergence *Gaussian* beam. The beam is divided in two mutually coherent waves by a semi-reflecting mirror (or a polarizing beam splitter cube). The reference wave is moving toward a fixed mirror where it reflects entirely. The probe wave is going toward the moving target, which partially reflects the incident wave. Both waves are put back together by the beamsplitter and then interfere. Both the incident and probe waves have instantaneous frequencies of respectively  $\nu_0$  and  $\nu_0 + \delta\nu_D$ ; Their interference is detected by a photodetector  $D$  localized in the interference field. The detection is maximal when both beams are parallel and perfectly covering the entire photodetector's surface. The tolerance of the angle  $\theta$  between both beams is defined by the following condition: the half interfringe  $i/2$  must be considerably higher than the diameter  $d$  of the photodetector. Under such conditions, the photodetector's lightning is almost consistent. The

angle  $\theta$  between both beams must respect  $\theta < \frac{\lambda}{2d}$ .

Numerical example:  $d = 1 \text{ mm}$  and  $\lambda = 633 \text{ nm}$ . The maximal angle between both beams is  $3 \times 10^{-4} \text{ rad}$ . Right outside the source, this angle has an order of magnitude of a HeNe (Helium-Neon) laser beam. With the right settings for the interferometer, the photodetector will be consistently lit.



In the event of wrong settings, the photodetector receives a medium light intensity, almost consistent, which prevents the detection of the contrasts between interferences.



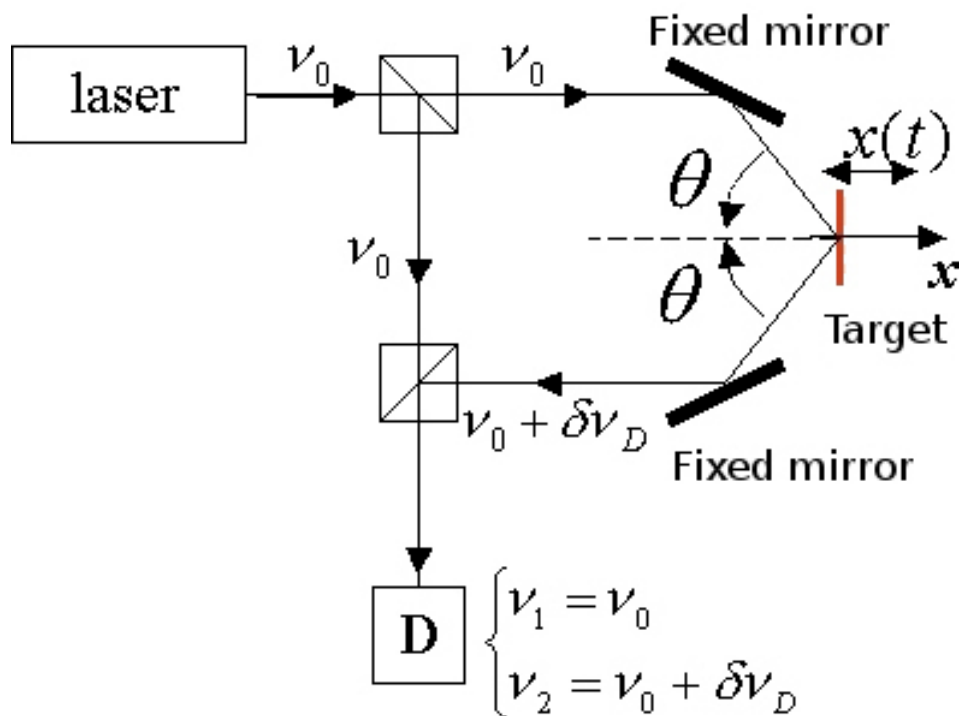
### Attention

In reality, laser sources are quasi-monochromatic. They are characterized by a line width  $\delta\nu$  which determines a coherence length  $L_c = c/\delta\nu$ . With a multimode HeNe laser having a line width  $\delta\nu = 2$  GHz, the coherence length is of 15 cm.

With a single mode laser having a line width  $\delta\nu = 1$  MHz, the coherence length reaches 300 m. This notion of coherence length is crucial in interferometry because it

defines the maximal path-length difference  $\Delta L \Delta L$  between two waves, in order to be able to see the interferences, which can be written as  $\Delta L < L_c$ .

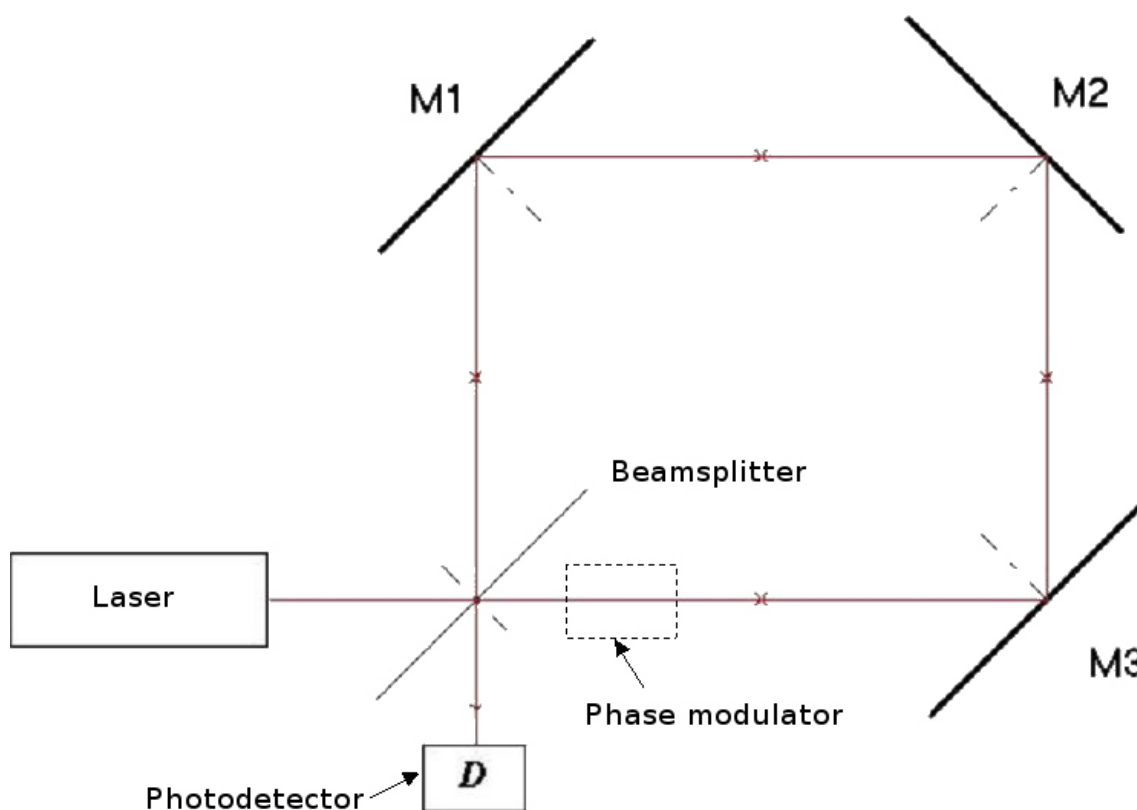
Figure 10 displays a Mach Zehnder interferometer where the moving target reflects a probe wave in oblique projection.



## Mach-Zehnder interferometer

In Michelson and Mach Zehnder interferometers, the optical elements must be rigorously attached in order not to induce any parasitic phase shifts by vibrating. Moreover, fluctuations in the path-length difference can be seen because of thermal perturbations on the reference and probe paths.

A third type of interferometer is the Sagnac one.



The beamsplitter divides the laser wave into two separate waves that go through the same path in opposite directions. Because of the waves' common path, this interferometer does not respond to slow random thermal perturbations, because both waves undergo the same phase shifts. To induce phase shifts in a Sagnac interferometer, there is a need for a phenomenon which will break the symmetry between both travel directions. This is what happens when the interferometer undergoes a rotation in the beams' plan. The Sagnac interferometer is at the root of fibre gyroscopes or gyrolasers. These instruments are designed to measure angular velocities and angular displacements.

The principle of the measurement of angular velocities using a Sagnac interferometer can be interpreted as the different Doppler shifts that both waves undergo, propagating in two opposite directions. For practical purposes, the interferometer is built with an optic fibre roll which gives a high propagation length (several hundred meters).

### Complément

The Sagnac interferometer can be used to make an optical-fibre ammeter. Indeed, an electric current makes a magnetic field around itself that is responsible for a magneto-optic effect in the fibre core: the **Faraday effect**. This effect can be considered as a circular birefringence phenomenon: the right and left circular polarised waves do not have the same phase velocities. If, inside the interferometer, the right and left circular polarised waves propagate in opposite directions and do not have the same phase velocity in the magnetic field, a phase difference appears between both waves after a short distance. This phase difference is proportional to the electric current intensity.

Finally, the propagation symmetry between both counter-rotating waves in a Sagnac interferometer can be broken if there is a phase modulator on the waves' path.

We will focus next on the interferometers able to measure sound and ultrasonic vibrations. They are built on the same basis of two-beam interferometers such as Michelson, Mach Zehnder, or a mixture of both types. Two types of interferometry will be distinguished: the *homodyne interferometry* and the *heterodyne interferometry*.

## 2. Homodyne interferometry

### 2.1. Definition

For practical purposes, both interferometer's waves are coming from the same laser frequency source  $\nu_0$ . The initial wave is divided in two by a semi-reflecting beamsplitter or polarising beam splitter cube. The two waves resulting from the amplitude's division are *coherent*. One of the waves, called *reference wave*, is directly in the direction of the photodetector without any frequency change. The second, know as *probe*, is reflected by the target and undergoes a Doppler shift before interfering with the reference wave near a photodetector.

#### Définition

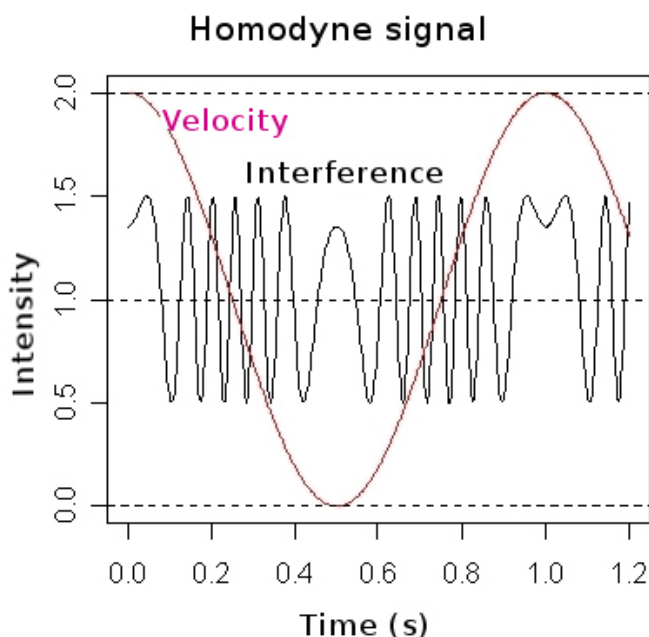
The interferometry is called *homodyne* when neither the reference wave nor the probe wave undergoes a frequency shift other than the Doppler shift happening on the target.

The instantaneous frequency of the interference signal is then:  $\nu_2 - \nu_1 = \delta\nu_D = \frac{\vec{v}(t) \cdot (\vec{e}_r - \vec{e}_{ij})}{\lambda}$ .  
If the path-length difference is small compared to the coherence length, then the interference

signal is  $I = I_0(1 + m\cos\Phi)$ , in which  $\Phi = 2\pi \frac{\Delta\vec{r}(t) \cdot (\vec{e}_r - \vec{e}_i)}{\lambda}$ .

#### Exemple

Figure 12 displays the typical signal of an homodyne interferometer when the target's displacement is a sinusoidal time function (red curve) with an amplitude equal to 3 times the wavelength.



### 2.2. Description of a homodyne Michelson interferometer

The optical setup displayed in figure 13 represents a homodyne Michelson interferometer.

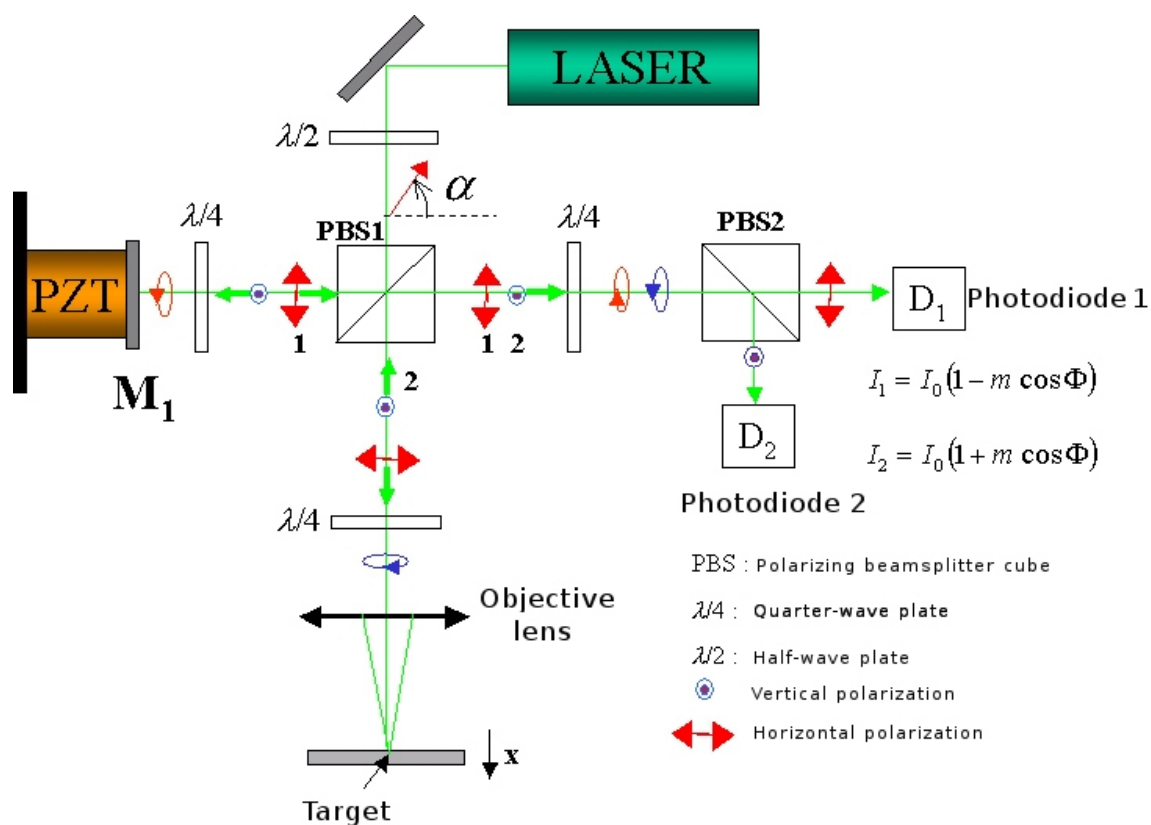
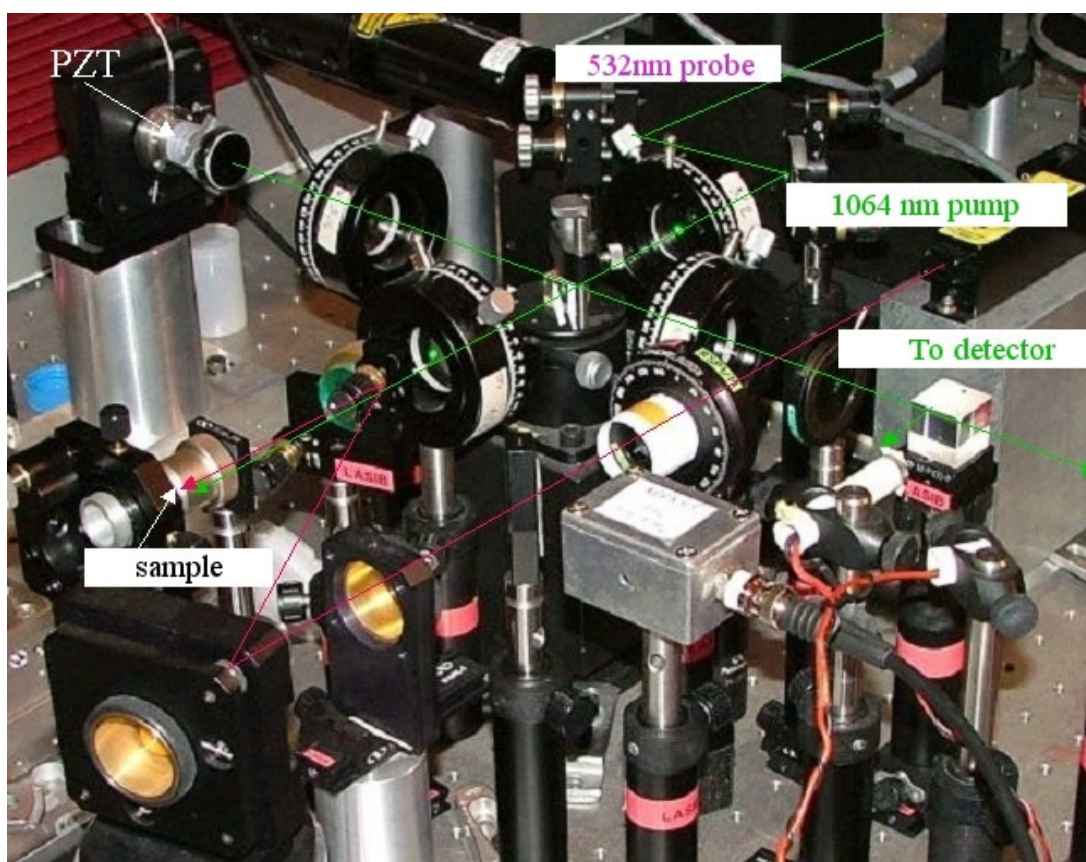


Figure 14 shows how to make the setup.



The linear polarization laser beam enters the interferometer through a half-wave plate  $\lambda/2$  which adjusts the polarization direction, before going through a polarizing beam splitter cube (PBS). The  $\lambda/2$  plate combined to the PBS regulates the sharing of the incident power  $P_L$  between the reference beam having a power  $P_1$  and the probe beam having a power  $P_2$ .

Assuming that the optical components do not lead to any kind of power loss, the conservation of the luminous power can be written as  $P_L = P_1 + P_2$ . How the beam distribution device works can be explained by the Malus law. The direction of the linear polarization at the entering of the PBS1 cube makes an angle  $\alpha$  compared to the horizontal direction. The PBS1 cube acts as a perfect polariser. The transmitted power is  $P_2 = P_L \cdot \cos^2(\alpha)$  whereas the reflected power is:  $P_1 = P_L \cdot \sin^2(\alpha)$ .

The wave (reference) reflected by a polarizing beam splitter cube is vertical and perpendicular to the incident plane (polarisation  $s$ ) whereas the transmitted wave (probe) has a horizontal polarisation parallel to the incident plane (polarisation  $P$ ). Then, the reference wave goes through a quarter-wave plate ( $\lambda/4$ ) whose neutral lines are 45° inclined compared to the horizontal and vertical directions. It reflects on the mirror  $M_1$  then goes back through the quarter-wave plate. Reflecting on a normal incidence mirror does not change the polarisation state. The traveling back and fourth through the quarter-wave plate changes the initial *linear vertical* polarization state into a final *linear horizontal* polarization state which will be entirely transmitted through the PBS1 polarising beam splitter cube.

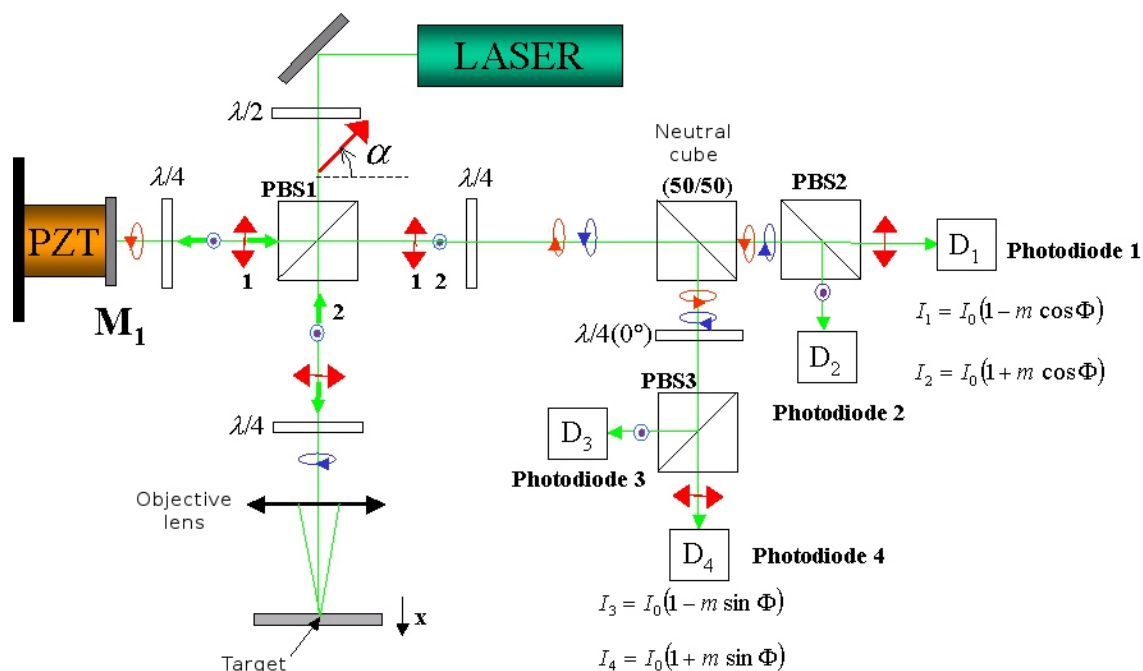
Identically, the probe beam goes through a quarter-wave plate which has the same orientation as the first one. It is reflected by the target and goes back through the quarter-wave plate. The traveling back and fourth through the quarter-wave plate changes the initial *linear vertical* polarisation state into a final *linear horizontal* polarisation state which will be entirely transmitted through the PBS1 polarising beam splitter cube. With this device, the beams cannot go back to the laser source, which, this way, cannot be destabilised. When using a laser diode as a light source, it is usually necessary to put an **optical isolator** right after the laser in order to avoid the light wave coming back to the laser. The photometric efficiency of this setup is maximal. The optical losses due to the reflection on diopters can be reduced to really low levels using optical elements having an antireflection coating.

After going through the PBS1, the reference and probe waves are collinear but their superposition does not lead to any type of observable interference because of their polarisation state being orthogonal. Thus, there is a need to project the polarisation states of both waves on a single polarisation state: at 45° of the horizontal and vertical directions with a polarising beam splitter cube inclined at 45°. The transmitted beam does not change direction whereas the reflected beam is inclined at 45° compared to the horizontal plan. We get two signals with opposite phases:  $I_1 = I_0(1 - m \cos\Phi)$  et  $I_2 = I_0(1 + m \cos\Phi)$ .

An alternative setup can be used. However, this one has the advantage of avoiding any beam going out of the working station. The alternative relies on putting a third quarter-wave plate right after the PBS1. This plate  $\lambda/4$  transforms both linear polarization states into two circular orthogonal polarisation states: right circular state and left one. The superposition or the interference of both the right and left circular states, having the same amplitude, results in a linear polarization state whose direction changes along the phase shifting of both circular waves. The interference signals detected by photodiodes  $D_1$  and  $D_2$  are:  $I_1 = I_0(1 - m \cos\Phi)$  and  $I_2 = I_0(1 + m \cos\Phi)$ .

### Remarque

If we want to find out the direction of the target's displacement using a homodyne interferometer, it is necessary to have at least two interference signals in quadrature ( $\Phi = \pm\pi/2$ ). This can be done by using the setup displayed in figure 15.



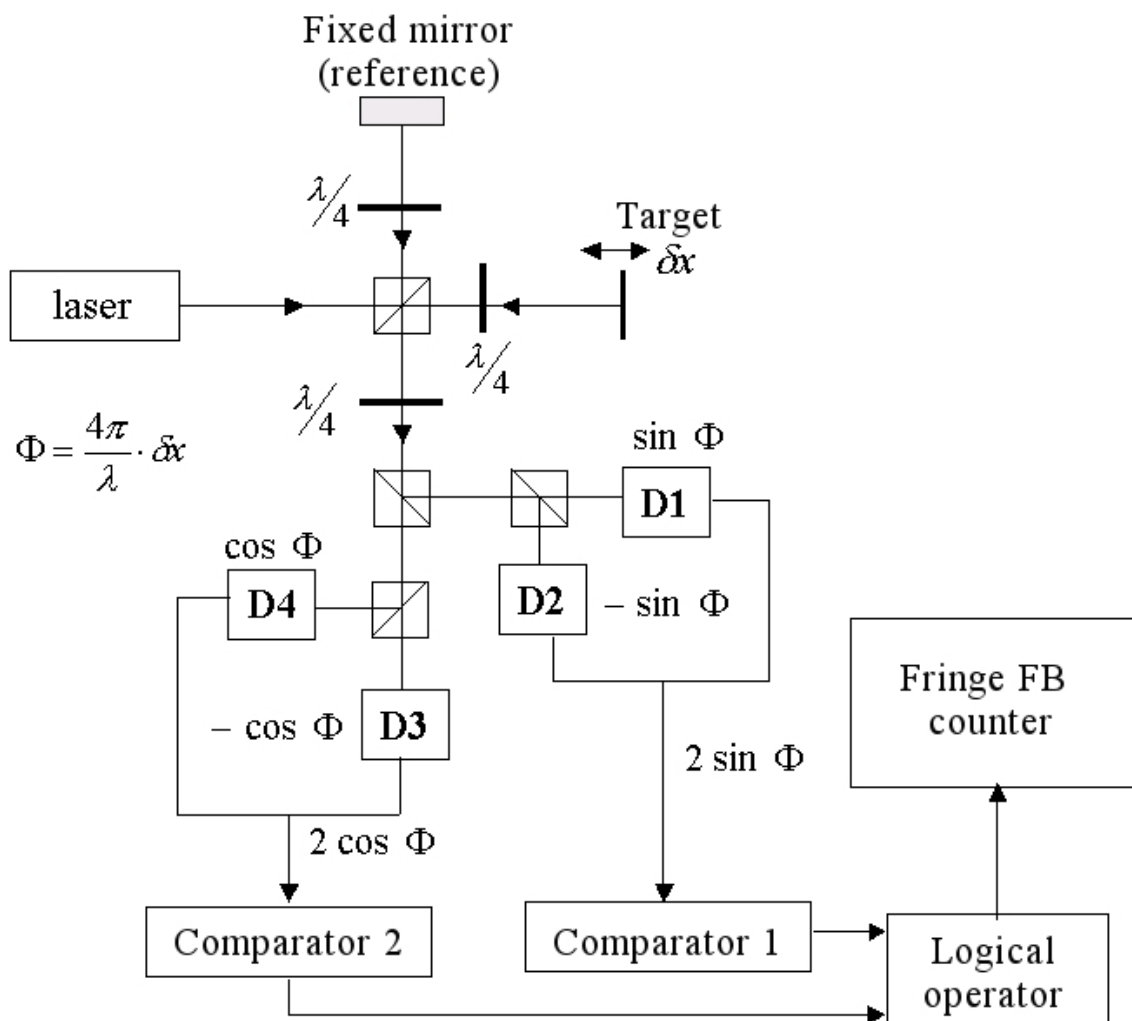
This last setup uses a fourth quarter-wave plate  $\lambda/4$  which changes the phases of both the reference and the probe waves by  $\pi/2$ . If we do not want to use an additional  $\lambda/4$  plate, we will then get the same result by putting the PBS3 at 45 compared to the horizontal direction.

The setup detection device depends on the resolution that we wish to reach on the displacement. We can distinguish three cases:

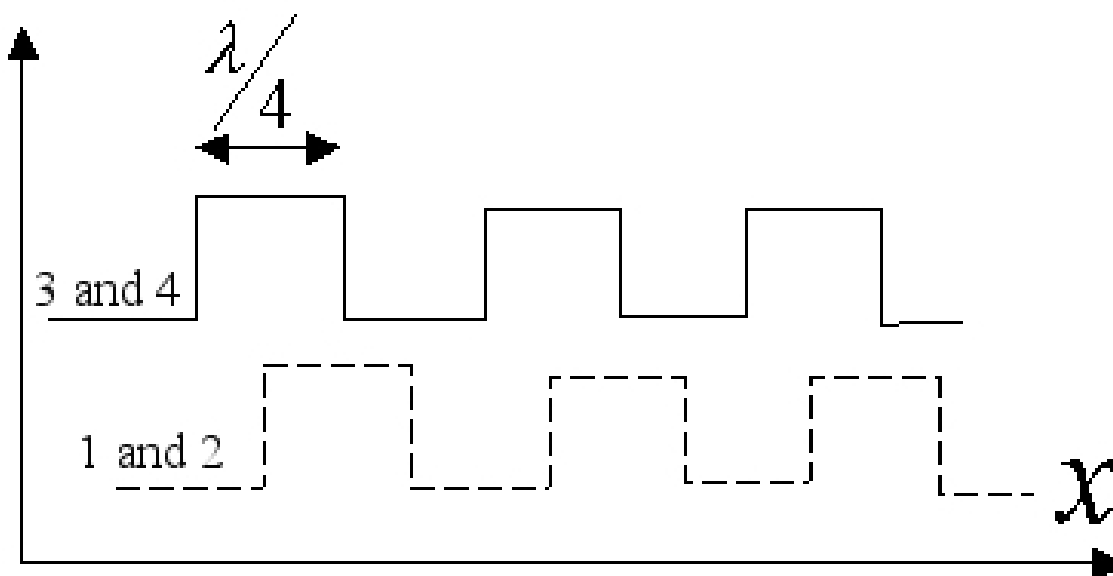
1. We wish to have a resolution between  $\lambda/8$  and  $\lambda$ . An *interference fringe counting system* will do the trick. The measuring range can go from a few centimeters to several dozens of meters, even hundreds of them. A fringe counting interferometer can be integrated to some *laser trackers*. These systems are used for three-dimensional and high precision metrology of large parts, such as planes'.
2. We are looking for a few nanometers resolution and the measuring range does not exceed a few micrometers. The displacement measurement needs a *phase demodulation* of the interference signal.
3. We want to make measurements with a resolution lower than the ultrasonic vibrations' nanometer which also have amplitudes lower than  $\lambda/8$  (refer to the case study). In this case, it is possible to directly get a linear response with the displacement by correctly choosing the interferometer's working point.

### 2.3. Displacement measuring using fringe counting

Figure 16 explains the principle of measuring a target's displacement  $\delta x$  by using a fringe counting system.



The device is made of four photodiodes. The beam that includes the superposition of both right and left circular polarizations is divided by a neutral cube which reflects 50% of the incident wave, transmitting the other half. A neutral cube does not change the waves' polarization state. Each of the beams created by this first division is then divided again in two new beams by a polarizing beam splitter cube. The currents delivered by each of the four photodiodes, proportional to the luminous powers received are:  $I_1 = I_0(1 + m \sin \Phi)$ ,  $I_2 = I_0(1 - m \sin \Phi)$ ,  $I_3 = I_0(1 - m \cos \Phi)$  and  $I_4 = I_0(1 + m \cos \Phi)$ , in which  $\Phi = 4\pi x/\lambda + \Phi$  represents the interference signal's phase. The photodiodes  $D_1$  and  $D_2$  on one hand, and the photodiodes  $D_3$  and  $D_4$  on the other, all plugged in series, are responsible for the differences between both currents:  $I_C = 2I_0 m \cos \Phi$  and  $I_S = 2I_0 m \sin \Phi$ . These last currents are converted into two tensions in quadrature, which make two basic comparators work. The logic level is equal to 1 if  $I_S, I_C > 0$  and equal to 0 otherwise. Both logical outputs in quadrature change depending on the displacement  $\delta x$  of the target.



Both logic signals, phase shifted by  $\pi/2$ , make fringe counting possible by using a FB counter.

### Remarque

The target's displacement direction can be determined by a fringe counting system and its minimal resolution  $\lambda/8$ . For a 633 nm wavelength of a HeNe laser:  $\lambda/8 \approx 80$  nm.

### Complément

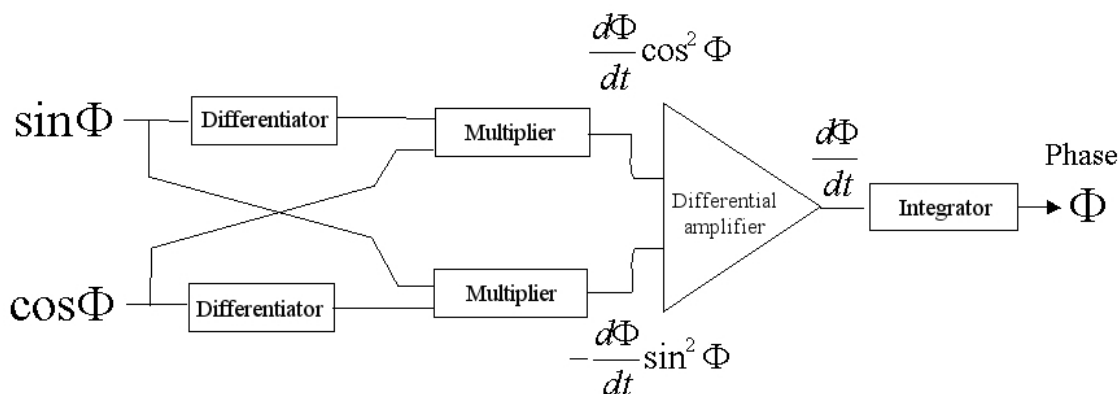
A *laser tracker* includes an error-free fringe counting interferometer. The interference signal's contrast must be continually close to a 100%. The probe beam cannot be attenuated when it reflects on the target, which can be several meters away from the interferometer. Thus, the target must be perfectly reflecting and has to send the probe laser beam in the same direction as the incident beam. These conditions are met if the target is a corner cube retroreflector. This reflector has the ability of sending back the reflected beam in the exact same direction as the incident beam. The operator holding the target does not have to worry about precisely sending the probe laser beam back toward the interferometer.

These conditions are met if the target is a corner cube retroreflector. This reflector has the ability of sending back the reflected beam in the exact same direction as the incident beam. The operator holding the target does not have to worry about precisely sending the probe laser beam back toward the interferometer. Moreover, a laser tracker includes a closed-loop control system of the probe laser beam which constantly follows the target. How much the probe beam is attenuated during the reflection is negligible if using an retroreflector, no matter how far the target is. However, the laser beam divergence is such that the contrast gets smaller and that the laser tracker's measuring range is limited. The laser source's coherence wave must be several dozen meters in order to maintain the contrast on the entire measuring range. Under true measuring conditions, the air temperature has to be quite homogeneous because it influences the optical index and thus the optical route. To find out more, go to:<sup>1</sup>

## 2.4. Demodulation of a homodyne signal

It is possible to get a better resolution than  $\lambda/8$  on a few wavelengths displacement by making a demodulation of the interference signal. In this case, it is necessary to replace the fringe counting system's comparators with an analogue demodulation setup, which uses both analogue signals in quadrature  $\sin\Phi$  and  $\cos\Phi$ .

1 - [https://knowledge.faro.com/Hardware/Laser\\_Tracker/Tracker](https://knowledge.faro.com/Hardware/Laser_Tracker/Tracker)



The demodulation can extract the phase  $\Phi$ , and thus the proportional displacement. The initial phase  $\Phi_0$  was considered up to here as constant but it can be influenced by thermal fluctuations, changes in pressure, etc. If we wish to measure displacements which are almost static, the interferometer must be built in a way that will minimize these external influences.

## 2.5. Measuring ultrasonic vibrations

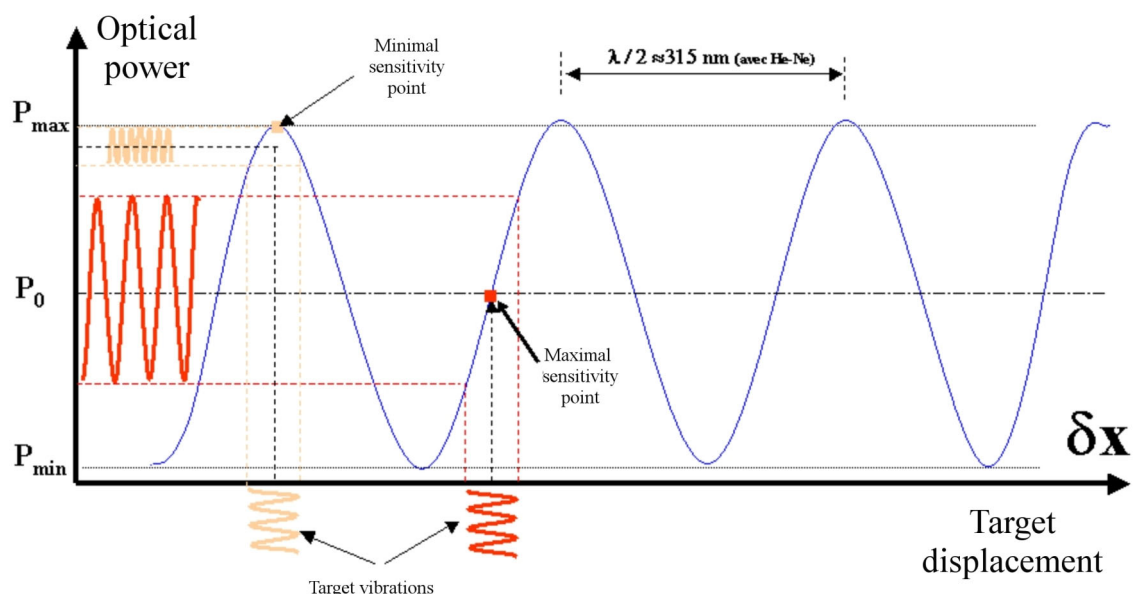
### a) Orders of magnitude

#### *Exemple*

The ultrasonic vibrations have low amplitudes, even more so compared to their high frequency. In a solid, the elastic waves can undergo deformations  $\eta$  whose amplitudes typically vary between  $10^{-6}$  and  $10^{-4}$ . With higher amplitudes, the non-linear phenomena threshold is reached, which can be destructive. The propagation velocity of a longitudinal acoustic wave in a solid or a liquid is usually around  $c = 5000\text{m/s}$ . The amplitude of particle velocities  $v$  is linked to the amplitude of the deformation by the relation  $v = c \cdot \eta$ . Thus, these particle velocities vary between  $5000 \times 10^{-6} = 5\text{ mm/s}$  and  $5000 \times 10^{-4} = 0.5\text{m/s}$ . The amplitude of particle displacements is linked to the amplitude of the velocity by the relation  $a = v/\omega$ , in which  $\omega$  is the vibration's beat. For a 20 kHz frequency, the lower limit of the ultrasound area, the matching vibration amplitudes are  $5 \times 10^{-3}/(2\pi \times 20 \times 10^3) = 40\text{ nm}$  and  $5 \times 10^{-1}/(2\pi \times 20 \times 10^3) = 4\text{ }\mu\text{m}$ . With 2 MHz, amplitudes range between and . Beyond 2 MHz, the vibration amplitudes are usually lower than than 50 nm. The phase demodulation system is no longer necessary. Under such conditions, it is possible to measure ultrasonic vibrations with a simplified demodulation system that we will present in the following paragraph.

### b) Measuring slight displacements: sensitivity of a homodyne interferometer

To measure displacements smaller than  $\lambda/8$ , there is a need to set the working point of the interferometer in a linear area.



We assume that the probe beam is backscattered on the surface of the target. The displacement  $\delta x$  that has been measured is the projection of the displacement on the sensitivity vector, which is collinear to the incident probe beam.

Figure 19 shows the sinusoidal variation of the interference signal (blue curve) according to the displacement  $\delta x$ .

The low amplitude sinusoidal vibration is represented in two cases:

- the interference signal is close to a maximum
- the signal is close to the peak of the curve

We can see on the illustration that the interferometer responds the most (i.e has the best sensitivity) in this latter case. Let's evaluate this sensitivity precisely.

$P_R$  and  $P_S$  refer to the reference and probe powers that light the photodetector.  $x$  represents the position of the target on an axis parallel to the probe beam. Then, the light power received

by the photodetector is

$$P = P_0 \left[ 1 + m \cos \left( \frac{4\pi}{\lambda} x + \Phi_0 \right) \right]$$

in which  $P_0 = P_R + P_S$  and  $m = \frac{2\sqrt{P_R P_S}}{P_R + P_S}$ .

The light power varies between  $P_{max} = P_0(1 + m)$  and  $P_{min} = P_0(1 - m)$ .

The *interference contrast* is  $m = \frac{P_{max} - P_{min}}{P_{max} + P_{min}}$  and the average power of the interference signal

is  $P_0 = \frac{P_{min} + P_{max}}{2}$ .

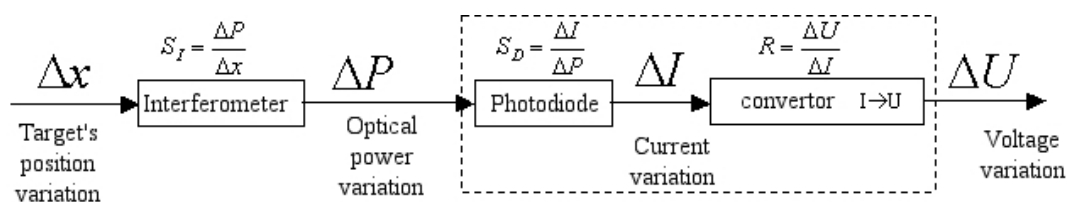
The sensitivity of the interferometer when measuring small displacements is defined by

$$S_I = \frac{\Delta P}{\Delta x} = \pm \frac{4\pi}{\lambda} P_0 m \sin(\Phi_0)$$

The maximal sensitivity can be acquired when the initial phase is equal to  $\phi_0 = \pi/2 + [\pi]$ . The interferometer must be locked in order to prevent thermal drifts of the phase  $\Phi_0$ . The maximal

sensitivity is  $S_I = \frac{\pm 4\pi}{\lambda} P_0 m$ .

The interferometer is the first step of the measuring chain which includes several blocks.



1. The interferometer transforms a position variation  $\Delta x$  into an optical power variation  $\Delta P$ ,
2. A photodiode converts the variation  $\Delta P$  into an electric current variation  $\Delta I$ ,
3. A transimpedance amplifier converts the current variation  $\Delta I$  into a voltage variation  $\Delta U$ .

The photodiode has a sensitivity  $S_D = \frac{\Delta I}{\Delta P}$ . The transfer function of the transimpedance amplifier in the bandwidth is  $R = \frac{\Delta U}{\Delta I}$ . We can group the last two steps of the chain in one single optoelectronic focus detection system:  $S_0 = \frac{\Delta U}{\Delta P} = \frac{\Delta U}{\Delta I} \cdot \frac{\Delta I}{\Delta P} = R \cdot S_D$ .

The global sensitivity of the chain when at its maximal sensitivity is:  $S = \frac{\Delta U}{\Delta x} = \frac{\Delta U}{\Delta P} \cdot \frac{\Delta P}{\Delta x} = R \cdot S_D \cdot \frac{4\pi}{\lambda} P_0 m$ .

### Exemple

With  $P_0 = 1 \text{ mW}$ ,  $\lambda = 532 \text{ nm}$ ,  $m = 1$ ,  $R = 10 \text{ k}\Omega$ ,  $S_D = 0.5 \text{ A/W}$  the sensitivity is equal to:  $S = R \cdot S_D \cdot \frac{4\pi}{\lambda} P_0 m = 10^4 \cdot 0.5 \cdot \frac{4\pi}{532 \cdot 10^{-9}} \cdot 10^{-3} \cdot 1 \approx 120 \text{ mV/nm}$

### Remarque

A photodiode's sensitivity is:  $S_D = \frac{\eta \cdot e \cdot \lambda}{h \cdot c}$ , in which  $\eta$  is the quantum efficiency,  $h$  the Planck's constant,  $e$  the charge of the electron and  $c$  the light velocity. The factor  $S_D/\lambda$  depends only on the quantum efficiency of the photodiode. Thus, the wavelength doesn't influence the sensitivity. However, the wavelength intervenes in the evaluation of the noise. The *signal-to-noise ratio* determines the smallest displacement that can be measured: it determines the resolution of the measuring instrument.

### c) Signal-to-noise ratio

In the measuring chain, the light source "photon noise" is the main source of noise. The photon noise has a quantum origin, because of the division of light energy into particles of energy  $h\nu$ : the photons. Therefore a luminous flux has to be considered as a discontinuous flux of photons, each of them being detected individually by a photodiode. In a given period and with a flow of photons being all constant on average, the number of photons detected is a random variable that follows the Poisson distribution.

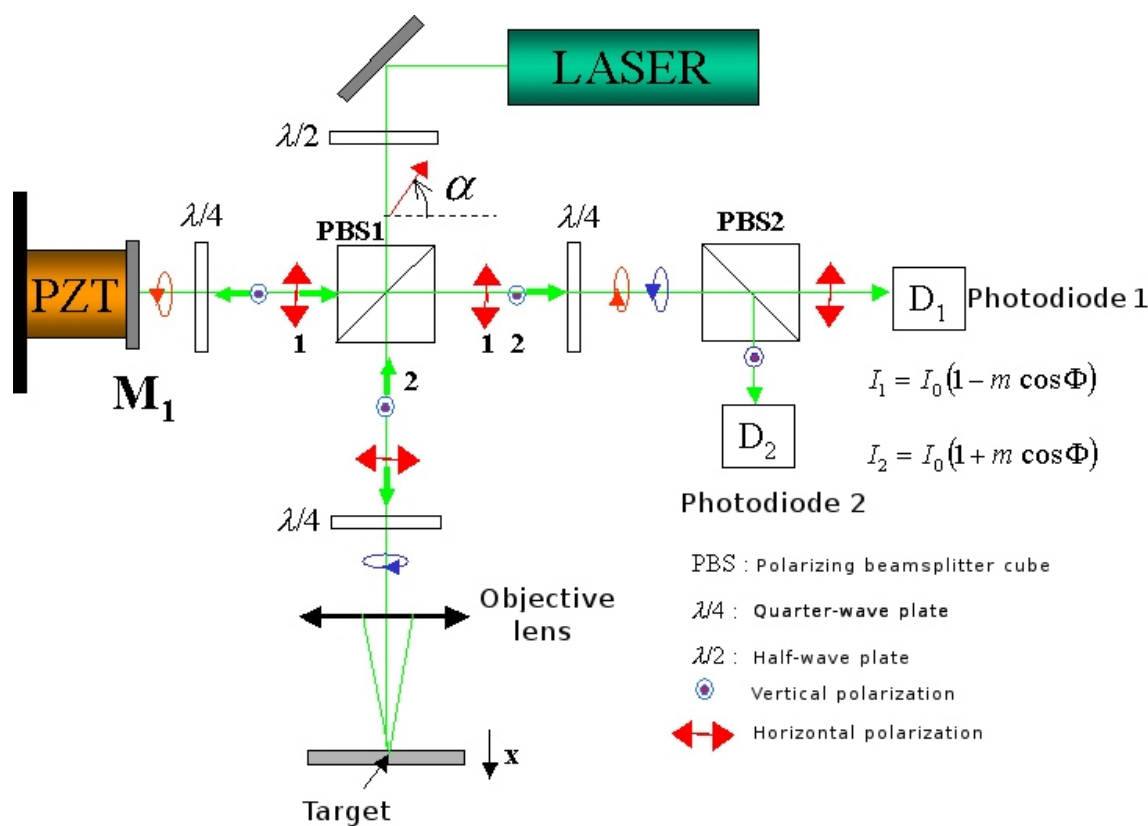
A second random process occurs when the incident photon is converted into a electron-hole pair, in the semiconductor junction. In practice, an incident photon is not detected with its 100% probability. A photon can either be detected or lost without being converted into a electron-hole pair. The quantum efficiency  $\eta$  of a photodiode expresses the probability of the detection process.

In the measuring chain, the signal conditioner of the photodiode, which includes the Johnson noise  $\sigma_U = \sqrt{4kT R \Delta f}$  in the resistor  $R$  of the transimpedance amplifier, constitutes the third source of noise. This noise can be ignored compared to the two first sources of noise.

Therefore the electrons are injected into the conditioning circuitry on a random basis. The resulting electronic noise is a “shot noise” type noise, in which the quantum of electric charge is the electron. The noise power spectral density of an electric current of average intensity  $\bar{I}$  is  $S_f = 2e\bar{I}$ . The standard deviation of current fluctuations in a bandwidth  $\Delta f$  is  $\sigma(I) = \sqrt{2e\bar{I}\Delta f}$ .

The “**photon noise**” should not be confused with the power fluctuations of the laser source, which are due to various instabilities within the emission process. Laser source manufacturers manage to make continuous-wave laser sources that have an excellent stability of emitted power. Nevertheless, the residual noise of the source is specified in a frequency band. For example, a value of 0.2% of 10 Hz to 1 GHz means that the standard deviation of the power fluctuations (RMS values) measured in the frequency band of 10 Hz to 1 GHz, equals 0.2% of the average power. This specification do not tell us how the noise is distributed in this band. Generally, a laser has a noise spectral density that decreases with the frequency, and that becomes negligible as soon as the frequency exceeds some MHz.

Let's consider that the homodyne interferometer of figure 21 is stabilised at the maximum sensitivity, so that it can detect ultrasonic vibrations of an amplitude of  $x(t)$ .



When a noisy laser source is present, the two interference signals can be written as follows

$$I_1 = [I_0 + i_B(t)] \cdot \left(1 - m \frac{4\pi x(t)}{\lambda}\right) \quad \text{et} \quad I_2 = [I_0 + i_B(t)] \cdot \left(1 + m \frac{4\pi x(t)}{\lambda}\right)$$

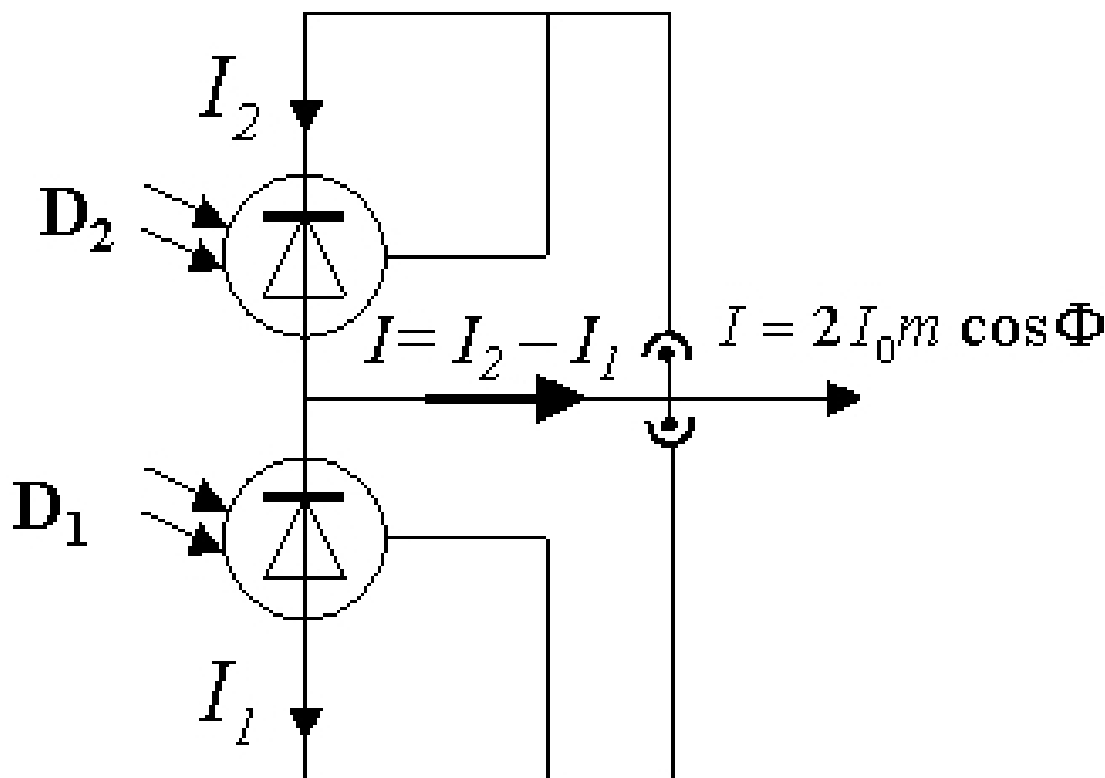
in which  $i_B(t)$  represents the fluctuations of the laser source, which is common to both ways of

detection. These fluctuations are low:  $i_B(t) \ll I_0$ . The currents are 
$$I_1 \approx I_0 + i_B(t) - \left[ I_0 m \frac{4\pi x(t)}{\lambda} \right]$$

and 
$$I_2 \approx I_0 + i_B(t) + \left[ I_0 m \frac{4\pi x(t)}{\lambda} \right]$$

The second common term  $i_B(t)$  that interferes with the interference signal can make it difficult to measure ultrasonic signals. The common interfering signal can be eliminated by subtracting the currents:  $I = I_2 - I_1$ .

The difference signal  $I \approx 2I_0m \frac{4\pi x(t)}{\lambda}$  now only includes the ultrasonic signal. The difference signal has the advantage of doubling the sensitivity, compared to the signal given by only one photodiode. The easiest way of subtracting the currents is to connect both photodiodes in series, as in figure 22.



In order to estimate the amplitude of these fluctuations, let's consider a series of integration time intervals  $\Delta t_i$  of the same length  $\Delta t$ . Let  $N_i$  be the number of electrons "counted" in each time interval  $\Delta t_i$ . The number  $N_i$  varies from an interval to the other. It has been established that the random variable  $N$  (the number of electrons counted in each interval  $\Delta t$ ) follows the Poisson distribution with an average value  $\bar{N}$ . This probability distribution is characterized by a

standard deviation  $\sigma(N)$  equal to  $\sqrt{\bar{N}}$ . The average intensity of the electric current is  $\bar{I} = \frac{\bar{N}}{\Delta t} e$ .

The standard deviation of the current fluctuations is  $\sigma(I) = \frac{\sigma(N)}{\Delta t} \cdot e = \frac{\sqrt{\bar{I}\Delta t}}{\Delta t} \cdot e = \sqrt{\frac{\bar{I} \cdot e}{\Delta t}}$ .

The integration time  $\Delta t$  which is the sampling period of the optical signal, is linked to the cutoff frequency  $f_c = 1/\Delta t$ .

According to the sampling theorem, the maximal bandwidth that can be reconstructed from the sampled signal is:  $\Delta f = \frac{f_c}{2}$ . In conclusion, the standard deviation of power fluctuations can be written as follows:  $\sigma(I) = \sqrt{2e\bar{I}\Delta f}$  (**Schottky formula**). The noise spectral density  $S_f = 2e\bar{I}$  is constant. The shot noise is a white noise.

As a first approximation, a photodiode can be modelled by a first-order low-pass filter, with a sampling frequency  $f_c$ . This frequency is linked to the rise time  $t_r$  from 10% to 90% of the current, for a gradual optical excitation:  $f_c \approx 0.35/t_r$ . In practice, in order to estimate its bandwidth, the photodiode is lighted up, without saturating it, by a short optical pulse representing a unit impulse. Its impulse response is measured: for a first-order system, it is a decreasing exponential function, whose time constant is  $\tau = t_r/\ln 9 = 1/(2\pi f_c)$ . For a photodiode, an equivalent noise bandwidth  $\Delta f \approx f_c$  is generally chosen.

The equivalent noise bandwidth of the complete measuring chain is determined by the stage with the smallest bandwidth.

### Exemple

A measuring chain includes: a photodiode, a transimpedance amplifier and an oscilloscope with respectively 2 GHz, 1 GHz and 20 MHz bandwidths. In this case, the equivalent noise bandwidth of the measuring chain is 20 MHz, the same as the oscilloscope's.

As a consequence, the noise power is proportional to the equivalent bandwidth of the measuring chain. The standard deviation of the fluctuations is proportional to the square root of this bandwidth. In order to estimate the signal-to-noise ratio just at the output of the transimpedance amplifier, let's postulate that the amplifier does not generate any additional noise (the noise factor is equal to 1). Thus the signal-to-noise ratio can be estimated at the current outlet of the photodiode.

### Définition

The signal-to-noise ratio for a displacement  $\Delta x$  is the quotient  $S/B = \frac{\Delta I}{\sigma(I)} = \frac{S_I S_D \Delta x}{\sqrt{2e\bar{I} \Delta f}}$ . With  $\bar{I} = P_0 S_D = P_0 \frac{\eta e \lambda}{hc}$ , the expression  $S/B = 2\pi m \sqrt{\frac{2\eta P_0}{hc\lambda \Delta f}} \times \Delta x$  can be found.

### Définition

The *noise equivalent displacement*  $\Delta x$  (NED) corresponds to the smallest displacement that can give a signal with an amplitude equal to the noise standard deviation. In other words, the SNR is equal to 1 (or 0 dB).

### Fondamental

**The noise equivalent displacement represents the smallest detectable displacement. It is the characteristic detection limit of the system, and it determines the resolution of the measure. The expression of the noise equivalent displacement is:**

$$\delta x = \frac{1}{2\pi m} \times \sqrt{\frac{hc\lambda \Delta f}{2n P_0}}$$

The definition of the *noise equivalent displacement* is similar to the definition of the *Noise Equivalent Power* (NEP) of the photodetector. The *detectivity* of the measuring system can be defined as the inverse of the NED.

### Exemple

The following calculation is made by taking up the data used to calculate sensitivity:

$$\frac{\delta x}{\sqrt{\Delta f}} = \frac{1}{2\pi m} \times \sqrt{\frac{hc\lambda}{2n P_0}} = \frac{1}{2\pi \times 1} \times \sqrt{\frac{6,62 \times 10^{-34} \times 3 \times 10^8 \times 532 \times 10^{-9}}{2 \times 1 \times 10^{-3}}} = 1,15 \times 10^{-15} \text{ m} / \sqrt{\text{Hz}} \approx 1 \text{ fm} / \sqrt{\text{Hz}}$$

The specific noise equivalent displacement is a characteristic parameter of laser Doppler vibrometers. When the bandwidth is equal to 1 MHz, the smallest detectable displacement is about of 1 pm, which represents the resolution of the measuring system. The *dynamic range* of

the laser Doppler vibrometer, which is the ratio between the largest measurable displacement in a linear system (about 100 nm, ( $\pm 50$  nm)), and the smallest measurable displacement (equal to 1 pm), equals  $10^5$ . In order to digitise the analogue signal on this dynamic range, an analogue-to-digital converter of at least 16 bits is required. Most of the digital oscilloscopes convert into 8 or 12 bits, which is insufficient.

A displacement of 1 pm is a value almost 10 times smaller than the average amplitude of the atomic vibrations, at room temperature. But despite all that, a laser Doppler vibrometer cannot detect atomic vibrations. In order to interpret such a measurement, the **measurement volume**, has to be taken into account: it corresponds to the volume of matter being probed by the laser beam. This volume is approximately equal to the product of the focused beam diameter by the light penetration depth into the material. The minimum diameter of the focused probe beam is in the order of the wavelength. Furthermore, the penetration depth  $\xi$  of the probe beam in a metal opaque matter depends on the complex optical index:  $n = n' - jn''$  and  $\xi = \lambda / (4\pi n'')$ , which is generally of 10 nm in a metal. The measurement volume is in the order of  $\lambda^2 \cdot \xi \approx 10^{-20} \text{ m}^3$  in a metal, with  $\lambda = 1 \mu\text{m}$ . The number of atoms in the measurement

volume is  $N = \frac{N_A \mu V_{mes}}{M}$ , in which  $N_A$  is the Avogadro constant,  $\mu$  is the density and  $M$  is the molar mass.

For aluminium, the number of atoms can be calculated as follows:

$$N = \frac{N_A \mu V_{mes}}{M} = \frac{6,02 \times 10^{23} \times 2700 \times 10^{-20}}{27 \times 10^{-3}} = 6,02 \times 10^8$$

The displacement measured is much larger than the average random thermal perturbation of the atoms' centre of mass  $N$ , which is  $\sqrt{N} \approx 25000$  times smaller than the individual atomic fluctuation. Therefore the fact of measuring displacements much smaller than the amplitude of atomic vibrations is not paradoxical, from the moment that a large group of atoms is measured.

With a laser source being powerful enough (it is quite easy to find continuous-wave, laser-diode-pumped, solid-state and double-frequency lasers at a wavelength of 532 nm, able to exceed 20 mW), it is possible to independently optimize the contrast  $m$  and the power  $P_0$ . First, the contrast is optimized by modifying the distribution of the optical powers between reference and probe beams. Then, by using an attenuator, the power  $P_L$  which is injected into the interferometer is adjusted to reach the saturation point of the photodetector.

### Exemple

Let's consider that the interferometer includes optical elements treated with an antireflection coating. Therefore the optical loss can be ignored. The incident power  $P_L$  of the laser is divided between the reference beam  $P_R = x \cdot P_L$  and the probe beam  $P_S^{incident} = (1 - x) \cdot P_L$  with a coefficient  $x$ . This power should remain below the threshold of destruction of the sample studied. The sample sends back to the detector a fraction  $S_C$  of the incident power:  $P_S = S_C \cdot (1 - x) \cdot P_L$ , where  $S_C$  is the backscattering coefficient of the target. The total power lighting up the photodiode:  $P_0 = P_R + P_S$  should be lower than a threshold value  $(P_0)_{max}$  which is in the order of some mW. With an excessive illumination of the photodiode, a linear response can no longer be guaranteed. Furthermore, it could be damaged definitively. Optimizing the SNR of the interferometer begins by setting the contrast  $m$  at its maximum value, by adjusting the power distribution between the reference beam and the probe beam. Then, the SNR should be optimised by increasing the power  $P_L$ , while being careful not to exceed the acceptable maximum value of the target and of the photodiode.

### Exemple

If the laser source is a small He Ne laser, the available power is generally lower than 2 mW. The most important thing to do is determine the distribution of the power  $P_L$  of the source between reference and probe, since it optimises the signal-to-noise ratio. At the photodiode level, the distribution of reference and probe powers are respectively equal to  $P_R = x \cdot P_L$  and  $P_S = S_C \cdot (1 - x) \cdot P_L$ . For a target with a given value of  $S_C$ , the optimisation of the signal-to-

noise ratio amounts to trying to find the value of the partition coefficient  $x$  which maximises the product  $m\sqrt{P_0}$ . It can be proven that this issue of optimization amounts to minimising the

function  $f(x) = \frac{1}{x} + \frac{1}{S_c(1-x)}$ . The optimum solution is  $x_{opt} = \frac{\sqrt{S_c}}{1 + \sqrt{S_c}}$ .

### Optimum SNR with $S_c=0.1$

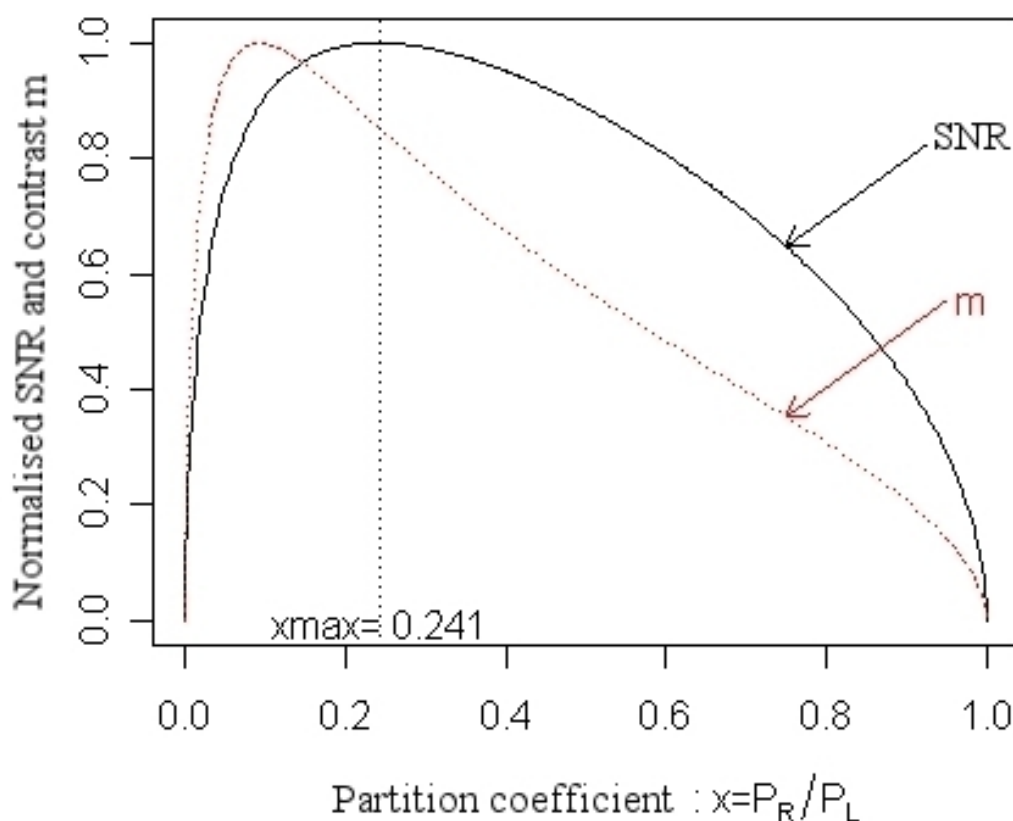
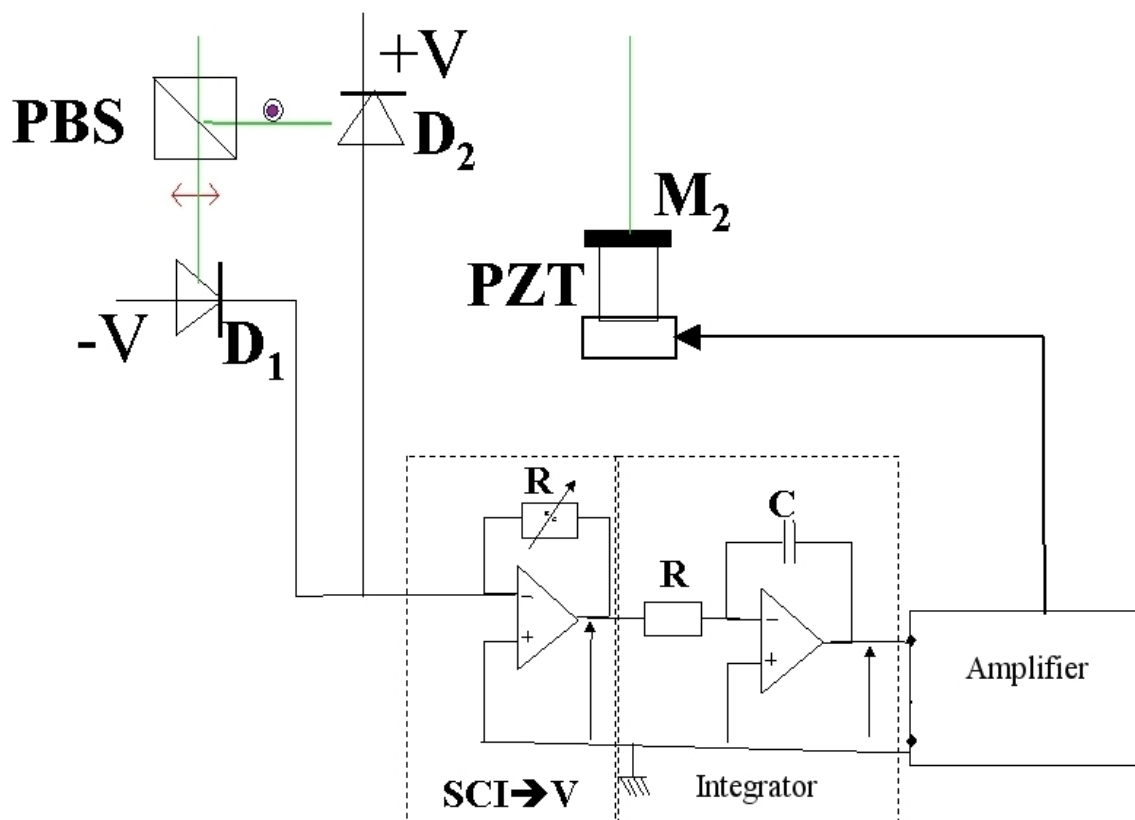


Figure 23 shows the evolution of the SNR and of the contrast  $m$  according to the partition coefficient  $x$  with a target sending back 10% of the incident power ( $S_c = 0.1$ ). In this case,

$x_{opt} = \frac{\sqrt{S_c}}{1 + \sqrt{S_c}} \approx 0,24$ . The SNR curve has been normalised according to its maximum.

#### d) Control of a homodyne interferometer in a closed-loop system

Air temperature drifts on the path of the beams. Vibrations of the interferometer's optical elements can cause interferences that modify the interferometric phase  $\Phi_0$ . In order to constantly maintain the sensitivity of a homodyne interferometer at its maximum setting, it is necessary to connect the interferometer to a closed-loop control system at the optimum working point. In practice, it can be made by fixing a mirror on a piezoelectric spacer (LZT), and by positioning it on the reference path. The position of the mirror is optimized by the voltage to which the spacer is subjected. Figure 24 ("Closed-loop control system") shows the diagram of the most appropriate simple closed-loop system to control the interferometer.



In practice, the stabilization of the interferometer can be maintained for several hours without any intervention from the operator if the environment of the interferometer is preserved from strong interferences. However, it is necessary to put the interferometer on an optical bench insulated from the vibrations of the ground and to preserve it from strong ambient convected air.

### Complément

How a closed-loop control system works: the error signal comes from two additional photodiodes  $D_1$  and  $D_2$  with a low bandwidth ( $\approx 1$  MHz) which take a negligible fraction (about 1%) of the luminous intensity. The luminous intensity is mainly sent to the fast photodiode  $D$  that detects ultrasound. The photodiodes  $D_1$  and  $D_2$  respectively get the powers

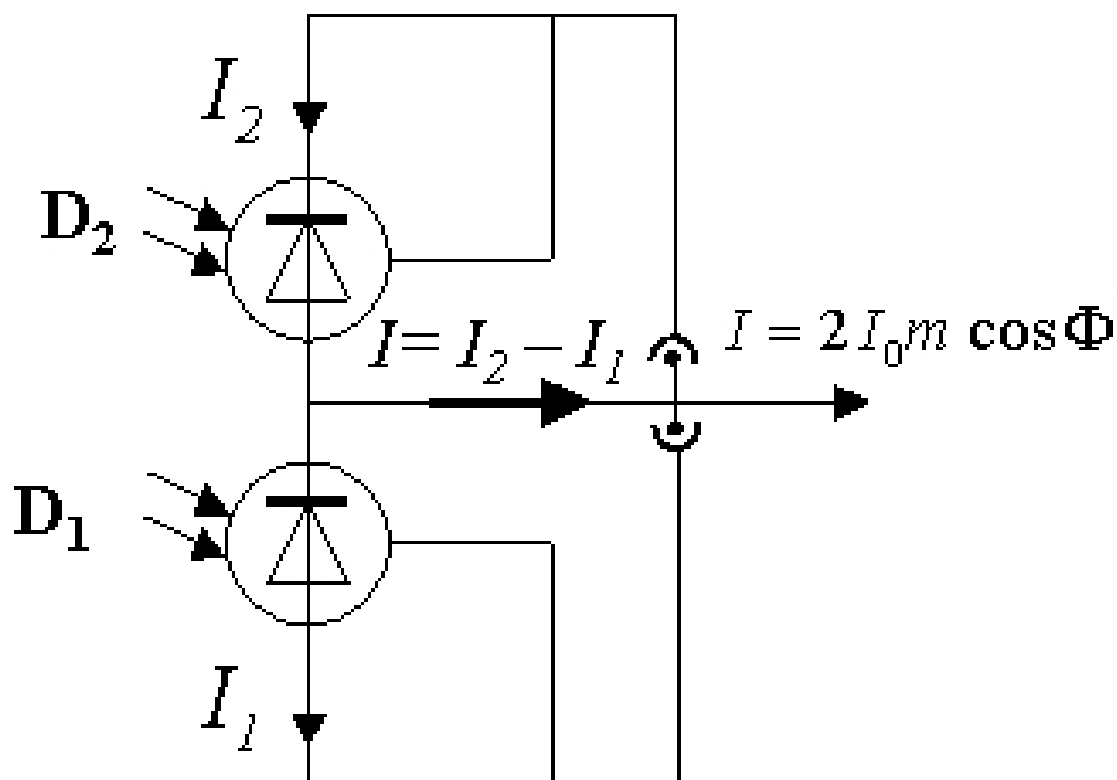
$$P_1 = P_0 \left[ 1 - m \cos \left( \frac{4\pi}{\lambda} x + \Phi_0 \right) \right] \text{ et } P_2 = P_0 \left[ 1 + m \cos \left( \frac{4\pi}{\lambda} x + \phi_0 \right) \right]$$

The currents generated by these two luminous fluxes are respectively:

$$I_1 = I_0 \left[ 1 - m \cos \left( \frac{4\pi}{\lambda} x + \Phi_0 \right) \right] \text{ et } I_2 = I_0 \left[ 1 + m \cos \left( \frac{4\pi}{\lambda} x + \phi_0 \right) \right]$$

The connection of both photodiodes in series generates a current  $I$  to the branch connecting the node common to both photodiodes, to the node located at the input of the transimpedance amplifier. This current is equal to the difference between the currents:

$$I = I_2 - I_1 = 2I_0 m \cos \left( \frac{4\pi}{\lambda} x + \Phi_0 \right)$$



The working point which gives the maximum sensitivity corresponds to a phase  $\Phi_0 = (2k + 1) \times (\pi/2)$ , in which  $k$  is an integer. The ultrasonic vibrations are of low amplitudes:  $x \ll \lambda$ . The term  $(4\pi/\lambda) \times x$  is always negligible before the phase  $\Phi_0$ . When the interferometer is controlled, the current  $I$  is zero. The piezoelectric spacer is modelled by a linear second-order system with a resonance frequency in the order of 1 kHz, and a damping constant  $\tau = 1$  ms. The closed-loop control system has a set of stable and unstable equilibrium states. Nearly in a state of equilibrium, the performance of the system can be compared to a linear second-order system. Only even (or odd) values of  $k$  give stable (or unstable) equilibrium states.

Modelling can be used to simulate the response to a phase interference  $\Phi_B$ , which is added to the phase interference  $(4\pi/\lambda).x$  of ultrasonic vibrations. The vibrations of the phase  $\Phi_B$  are much slower than the phase vibrations coming from the term  $(4\pi/\lambda).x$ . Simulating the response to a gradual phase interference  $\Phi_B$  makes it possible to set the parameters of the closed-loop control system. The aim is a return to equilibrium, with a response time as short as possible and without any oscillating response. An optimum response time depends on the damping constant of the piezoelectric spacer. A response time in the order of 10 ms can be suitable to offset thermal drifts and air turbulences. The closed-loop control system performs like a high-pass filter with a sampling frequency close to 100 Hz. Therefore ultrasonic frequencies are not reduced by the closed-loop control system.

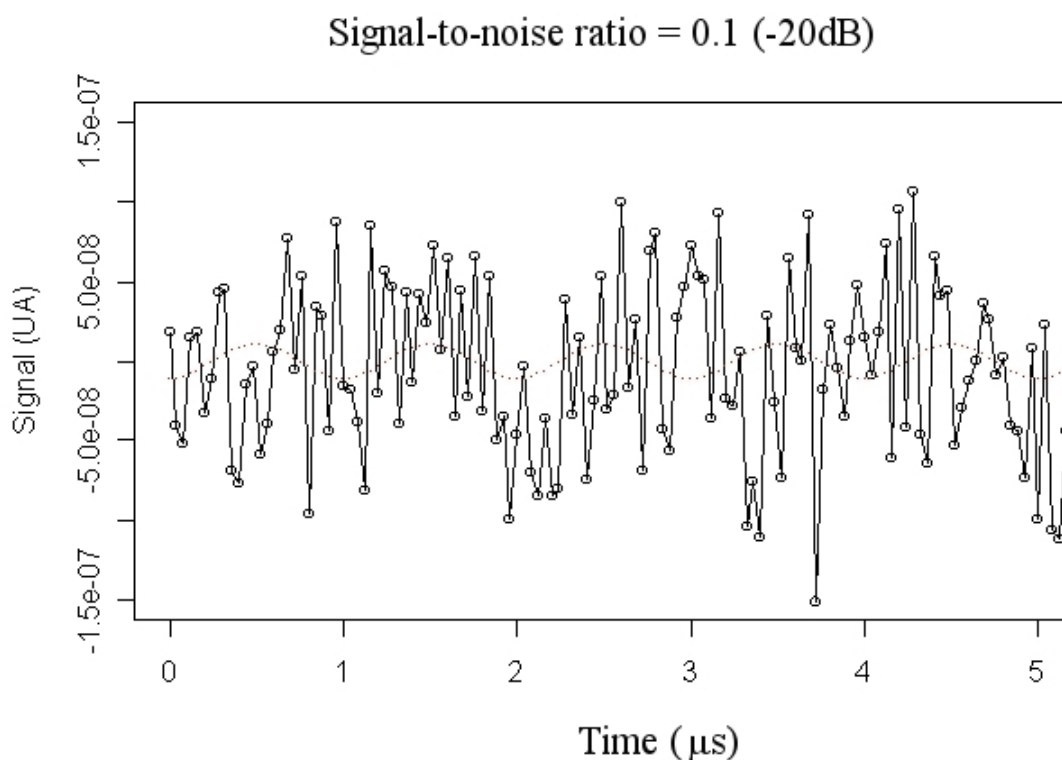
### e) Improving the signal-to-noise ratio of a repeated signal

It is not unusual for the ultrasonic signal to be measured to have a negative signal-to-noise ratio (in dB). If the studied phenomenon is not repeated, it will be impossible to extract the transient ultrasonic signal from only one acquisition. On the other hand, if it is a sinusoidal

steady-state phenomenon, it will be possible to extract the amplitude of the sinusoidal signal from the spectrum, by using a Fourier transform. The white noise is uniformly distributed on the spectral range, whereas the signal (which is concentrated on a narrow part of the spectral range) will be able to emerge from the noise.

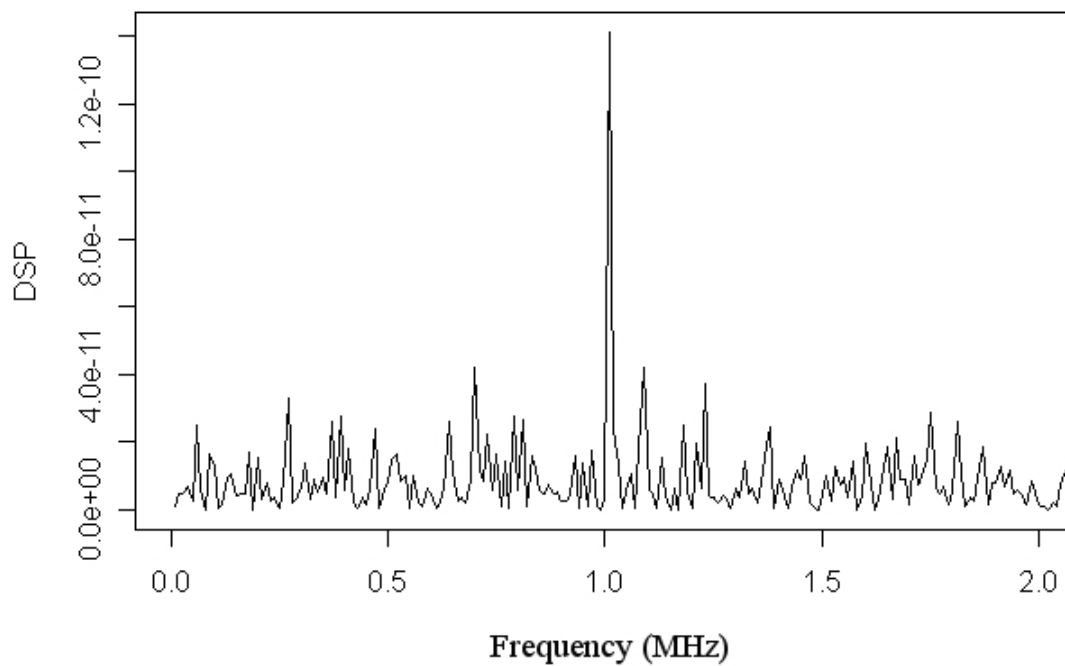
### Exemple

Let's consider a steady-state sinusoidal signal with an amplitude 10 times lower than the RMS value of the noise ( $SNR = -20$  dB) and with a frequency of 1 MHz. The cutoff frequency is of 25 MHz. This typhic noisy signal is represented on figure 26.



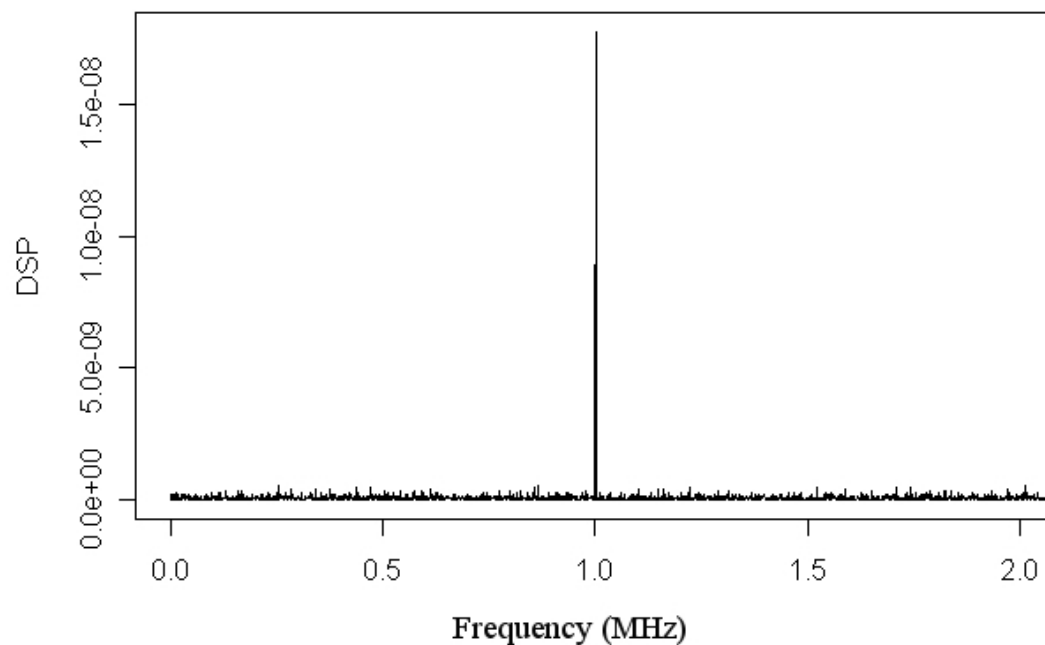
With a small number of periods, it is impossible to determine the amplitude of the sinusoidal signal, lost in the noise. On the other hand, if the acquisition of the signal is repeated during 100 periods, the signal emerges from the noise in the spectral range. The calculation of the fast Fourier transform gives the spectrum of figure 27. The vertical scale represents the **P**ower **S**pectral **D**ensity (PSD).

## FFT of a signal of 0.1ms (100 periods)



In the spectral range, the signal will emerge even more from the noise if the sinusoidal oscillation is constant during 1,000 periods (representing 25,000 points) (figure 28).

## FFT of a signal of 1ms (1,000 periods)



If the signal is a superimposition of several sinusoidal oscillations slightly dampened, with quality factors  $Q \approx 1000$ , it is possible to extract the different frequencies that make up the signal.

When the ultrasonic signal that you want to measure is a short transient one, it is necessary to try to repeat the phenomenon, and to average as many repetitions of the transient phenomenon as possible.

Each acquisition should be synchronised with a trigger signal. When the ultrasound is produced by a pulsed laser (pump), the "pumping" light pulse acts as a trigger signal. The acquisition system can be a digital oscilloscope with a *signal averaging function*. This "averaging" function generally improves the vertical resolution of the oscilloscope, which can increase from 8 to 16 bits. The SNR out of the averaged signal increases by  $1/\sqrt{N}$  of the number  $N$  of acquisitions. With a digital oscilloscope able to acquire and to average thousands of signals, it becomes possible to detect vibration amplitudes of 1 pm, in a bandwidth of 1 GHz, and with a signal-to-noise ratio greater than 20(+26 dB), that is to say a NED in the order of 50 fm (see case study).

### Exemple

If the noise equivalent displacement for an acquisition is of 1 pm, the average of  $N = 100$  acquisitions will give a NED equal to 0.1 pm. Figure 28bis shows the simulation of a signal superimposed to a Gaussian noise with a standard deviation equal to the unit (blue curve), compared to the signal averaged 100 times (red curve). For the simulation, the cutoff frequency of the signal is of 50 per arbitrary time unit.

### Complément : Calculation of the noise variance in an averaged signal

Each signal is sampled with a certain frequency  $f_e$  for a duration  $\Delta t$  and contains  $N_e = f_e \Delta t$  samples at the moments:  $t_j, j = 1, \dots, N_e$ .

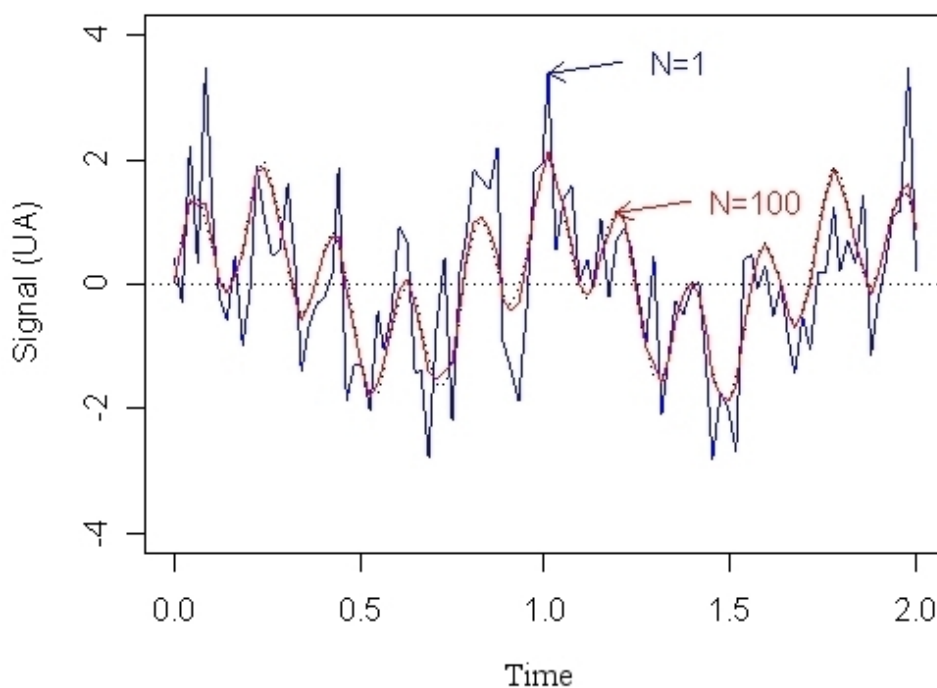
Each one of the  $N$  signals  $s_i(t_j), i = 1, \dots, N$  can be considered to be the sum of the ultrasonic signal  $s_0(t_j)$  (which is considered to be constant at each repetition) and of a random signal  $b_i(t_j)$ . The average of  $N$  random signals tends to a zero signal when  $N$  tends to infinity. In other words, a random signal is a *random variable* with a zero expected value:  $E[b(t)] = 0$ , whatever the moment  $t$ . Each random signal characterised by a variance independent from the moment  $t_j$  :  $Var[b] = \sigma_b^2$ , where  $\sigma_b$  represents the standard deviation of the noise. Let's calculate the noise variance on the averaged signal:  $\bar{s}_i(t_j) = \bar{s}_0(t_j) + \bar{b}_i(t_j) = s_0(t_j) + \bar{b}_i(t_j)$ .

The  $N$  random signals are statistically independent, therefore the variance of the sum  $\sum_{i=1}^N b_i(t_j)$  is equal to the sum of the variances of each term of the sum. Hence

$$Var[\bar{s}] = \frac{1}{N^2} \sum_{i=1}^N Var[b_i] = \frac{1}{N^2} \sum_{i=1}^N \sigma_b^2 = \frac{1}{N} \sigma_b^2.$$

The standard deviation of the noise on the averaged signal is equal to  $\sigma[\bar{s}] = \frac{\sigma_b}{\sqrt{N}}$ . The standard deviation of the noise decreases by  $1/\sqrt{N}$ , where  $N$  is the number of acquisitions.

Noisy signal ( $\sigma_b = 1$ ): Averaged ( $N=100$ ) and unaveraged ( $N=1$ )

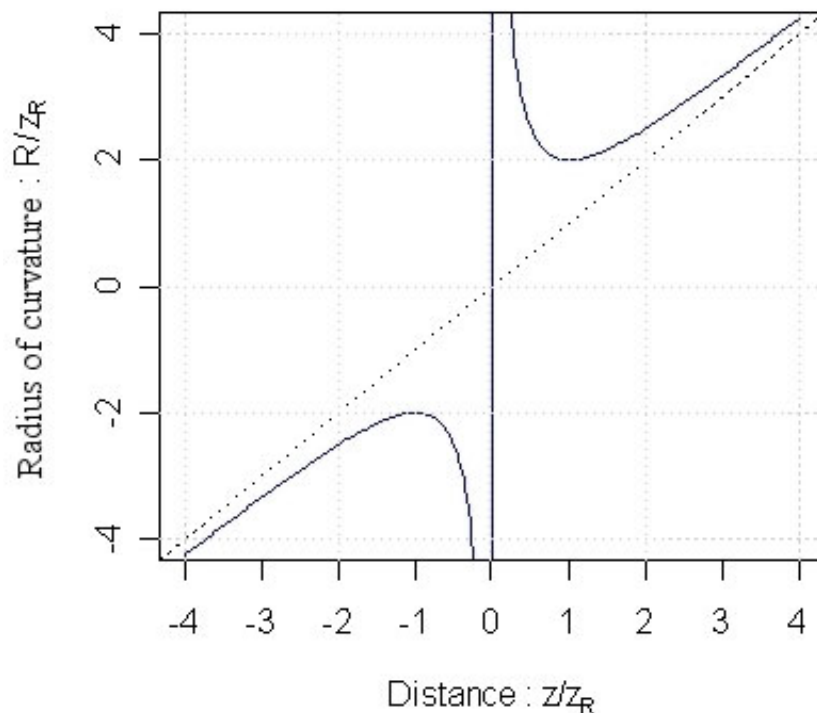


#### f) Focusing on a spherical target

When the studied surface is curved, the incident probe beam should be focused on the target so that it allows the recollimation of the backscattered light. Otherwise, the performances of the interferometer would be sharply reduced.

This recollimation happens when the curve of the wave front is equal to the curve of the target. The focal length  $f$  of the objective should be chosen so that the radius of curvature of the surface is greater than the minimum radius of curvature of the wave.

Let  $w$  be the Gaussian beam radius before the objective. The radius of curvature  $R$  of a focused Gaussian laser beam goes through a minimum value equal to  $2z_R = (2\pi w_0^2)/\lambda$ , where  $z_R$  is the Rayleigh distance of the focused laser beam, and  $w_0 = (\lambda f)/(\pi w)$  the waist of the laser beam.



Let  $R_{cible}$  be the radius of curvature of the spherical target. The recollimation condition of the probe beam is  $R_{cible} > R_{min} = (2\pi w_0^2)/\lambda = (2\lambda/\pi) \cdot (f/w)^2$ . In order to minimise  $R_{min}$ ,  $w$  should be increased, the beam should be widened so that it covers the whole aperture of the objective.

### Exemple

Let  $w_{max}$  be the aperture radius of the Gaussian beam in the objective and  $NA = w_{max}/f$ , the numerical aperture of the objective. The minimum radius of curvature is  $R_{min} = (2\lambda/\pi)/NA^2$ . With  $\lambda = 532 \text{ nm}$  and  $NA = 0.2$ ,  $R_{min} = 17 \mu\text{m}$ . Therefore it is possible to focus the beam on a target with a radius of curvature  $\approx 20 \mu\text{m}$ .

### g) Importance of the numerical aperture of the objective

Let  $S_C$  be the *scattering coefficient*, that is to say the fraction of power backscattered by the target. The "borderline case" of a perfectly reflective target corresponds to  $S_C = 1$ . On a black and scattering surface,  $S_C$  is close to 0.

This scattering coefficient depends on two parameters:

1. the albedo  $\alpha$  of the target
2. the numerical aperture  $NA$  of the objective.

The total luminous intensity sent back by a Lambertian scattering target into  $2\pi$  steradian is  $P_S^d = \alpha P_S^i$ , where  $P_S^i$  is the probe incident power. The intensity scattered into  $2\pi$  steradian is isotropic. The scattered luminous intensity that goes back to the objective is proportional to the solid angle of aperture of the objective  $\Omega \approx \pi NA^2$ . The backscattered power is  $P_S = P_S^d \frac{\Omega}{2\pi} = \alpha \frac{NA^2}{2} \cdot (1-x)P_L$ . Thus, the scattering coefficient is  $S_C = \alpha \frac{NA^2}{2}$ . Therefore

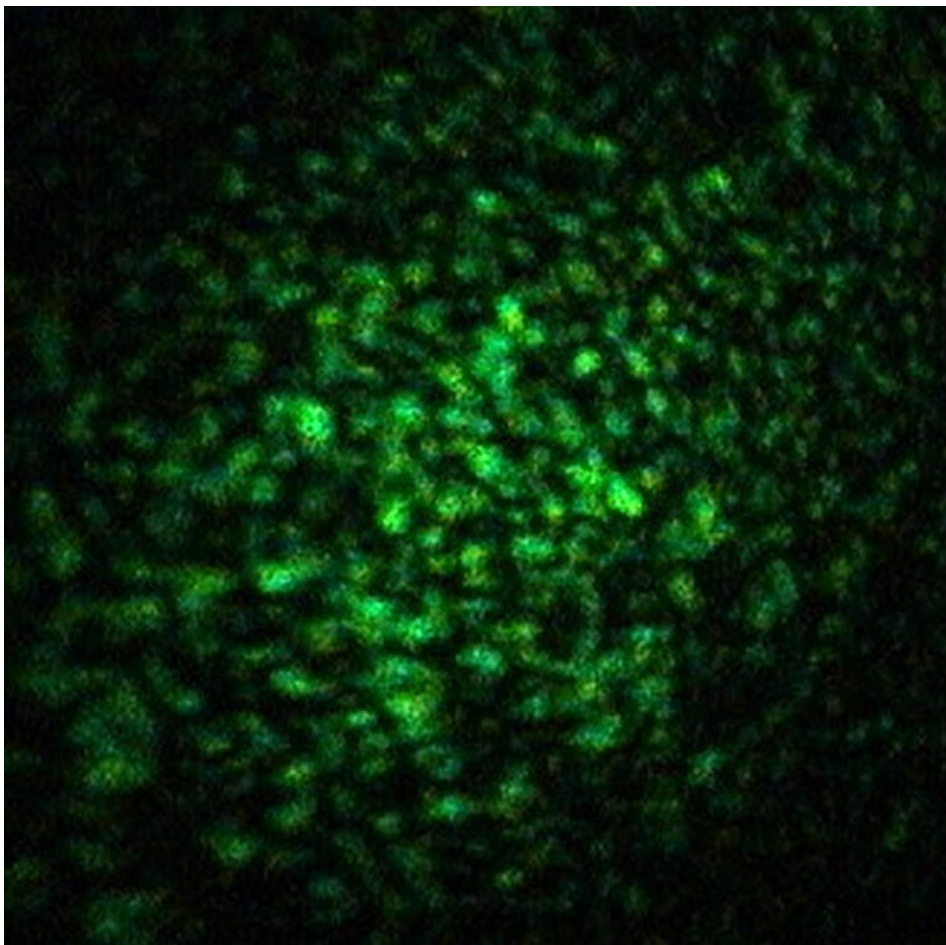
using a high numerical aperture objective improves the performances of the laser Doppler vibrometer.

### Exemple

The light scattered by a grey target with an albedo  $\alpha = 0.1$  is collected by an objective with a numerical aperture  $NA = 0.2$  and gives a scattering coefficient  $S_C = 2 \times 10^{-3}$ .

### Remarque

With a laser beam, the coefficient  $S_C$  can be greater than the value  $S_C = \alpha \cdot NA^2 / 2$  because of the "speckle" effect. In the "speckle" pattern, the luminous intensity has a random distribution between an almost zero value (between the grains of "speckle") and a value equal to twice the average value on a grain of "speckle".



The speckle phenomenon has two characteristics:

1. When the focusing is perfectly aimed on the target, the average divergence of a grain of speckle is equal to the divergence of the probe beam before (and after) the objective. The grain of speckle recollimated by the objective has an average diameter equal to the diameter of the incident laser beam. This diameter is a maximum. When the backscattered beam is not perfectly recollimated by the objective, the average size of the grains is smaller than the diameter of the incident beam. This observation offers a practical device to focus on the scattering surface.
2. The speckle pattern varies continuously when the area lit up by the laser beam is modified. As a result, to obtain a maximum interference signal, the position of the target should be adjusted to place a grain of speckle in coincidence with the probe

beam. The “hunt” for the grains of speckle makes it possible to increase the signal-to-noise ratio of the interferometer.

### Remarque

In the connection used in LDA or in surface velocimetry, the objective has a numerical aperture much greater than the divergence of the probe beams, which are focused on the target. The photodetector collects numerous grains of “speckle”.

## 2.6. Advantages and drawbacks of the homodyne interferometer

The advantage of the homodyne interferometer is its almost unlimited bandwidth and its sensitivity independent of the frequency. Only the photodetectors can limit the bandwidth. In theory, it is possible to measure ultrasound at frequencies of some GHz with a homodyne interferometer.

However, there is a limit to the detection of high frequencies for two reasons:

1. Beyond 1 GHz, the vibration amplitudes rarely exceed some dozens of picometers,
2. The noise increases proportionally to  $\sqrt{\Delta f}$  where  $\sqrt{\Delta f}$  is the bandwidth. Therefore the signal-to-noise ratio decreases rapidly when the frequency increases.

To measure ultrasound with a homodyne interferometer, a closed-loop control system is necessary to stabilize the working point at its maximum sensitivity. The homodyne interferometer is very sensitive to the disturbances of its environment (vibrations, thermal fluctuations), which can lead to drifts of the working point. These drawbacks can be minimized by positioning the interferometer on an optical bench, which insulates the interferometer from the vibrations of the ground. All these elements limit the use of such a measurement system to the preserved environment of a laboratory.

In disturbed environments, in an industrial setting or outdoors, the large majority of measurements are carried out with laser Doppler vibrometers. Furthermore, a very high bandwidth is not always necessary. Thus, for a particular application, the bandwidth should be restricted. This is the case for most interferometers included into industrial instruments: laser Doppler vibrometer, laser tracker, LDA sensor, etc. These are based on *heterodyne interferometers*.

\* \*  
\*

To know more about it, please consult the following references: (1 [[1]],2 [[2]],3 [[3]],4 [[4]],5 [[5]])

## II. Case study

### 1. Measurements of ultrasonic vibrations up to 1GHz

This case study will focus on the results of ultrasonic vibration measurements, obtained with a stabilized homodyne Michelson interferometer. The studied sample is a 500 nm-thick gold film positioned on a silicon substrate, with the aim of carrying out a study of the film/substrate interface. Ultrasonic vibrations are excited by “thermoelastic effect”, by using a passively Q-switched Nd:YAG microchip laser, which emits short pulses in the near infrared at 1,064 nm. This laser is called a “pump” laser. Each pump pulse has a duration of  $\tau_L \approx 1$  ns and an energy of  $E_L \approx 10 \mu\text{J}$ , and is focused on the sample, on a  $100 \mu\text{m}$ -diameter spot.

The thermoelastic effect mechanism on the metal surface can be explained as follows: a part of the pump energy is absorbed in the absorption thickness of the metal, which is generally of 10 nm. During the laser pulse, the heat diffusion takes place on a characteristic thickness of thermal diffusion  $e = \sqrt{D \times \tau_L} = \sqrt{(1,2 \times 10^{-4} \times 10^{-9})} \approx 350$  nm, where  $D$  is the thermal diffusivity of gold. The heating of this thin film results in a rapid thermal expansion, which causes a deformity pulse. As the environment is elastic, the interference propagates into the film in the form of a pulsed ultrasonic wave.

The ultrasonic wave is partially reflected, and transmitted to the film/substrate interface, which leads to a mitigation of the ultrasonic waves in the film, in a duration lower than  $1 \mu\text{m}$ . The pulse train of the pump laser makes it possible to repeat the phenomenon at a rate of about 10 kHz, ie one acquisition every  $100 \mu\text{s}$ . The ultrasonic signals provide information about the nature of the film/substrate interface.

The probe laser of the interferometer is a continuous-wave, diode-pumped, solid-state laser at 532 nm. The probe beam is focused on the film, with an objective of focal length  $f = 8$  mm. The Gaussian laser beam, which has a radius of  $w = 1.5$  mm before the objective, is focused on

$$w_0 = \frac{\lambda f}{\pi w} = \frac{532 \times 10^{-9} \times 8 \cdot 10^{-3}}{\pi \times 1,5 \times 10^{-3}} = 0.9 \mu\text{m}$$

a focus spot with a Gaussian radius of

This spot is at the centre of the focus point of the pump beam. The maximum contrast of the interferences is reached when the sample is positioned in the focal plane of the objective.

The detection of interference signals requires a photodetector with two outlets: a DC outlet for low-frequency signals from 0 to 30 kHz, and an AC outlet for high-frequencies signals from 30 kHz to 1 GHz.

In order to determine the sensitivity of the interferometer, the average incident optical power  $P_0$  and the contrast  $m$  of the interferences should be measured. The characteristics of the probe laser and of the photodetector, as well as the measuring conditions are presented in the table below.

Wavelength of the probe laser	532nm
<b>PHOTODETECTOR with a DC and an AC outlets</b>	
Sensitivity of the Silicon PIN photodiode at 532 nm	0.3A/W
Current-to-voltage conversion (DC outlet)	10000V/A
Current-to-voltage conversion (AC outlet)	700V/A
Bandwidth of the AC signal	30kHz -1GHz
<b>Measuring conditions of the interferometer</b>	
DC voltage at the minimum / maximum of interferences	1.7V / 7.3V

First, the interferometer is not controlled (open-loop system) and the mirror of the reference arm is set in oscillation thanks to a low-frequency sinusoidal voltage on the piezoelectric

actuator that supports the mirror. The optical power variations appearing on the photodetector result in voltage variations on the DC outlet. The minimum voltage  $U_{min}$  and maximum voltage  $U_{max}$  are recorded: they are proportional to the incident powers  $P_{min}$  and  $P_{max}$  on the photodetector.

$$m = \frac{P_{max} - P_{min}}{P_{max} + P_{min}} = \frac{U_{max} - U_{min}}{U_{max} + U_{min}} = \frac{7,3 - 1,7}{7,3 + 1,7} = 0,622$$

The contrast and the average flux  $P_0 = \frac{P_{max} + P_{min}}{2} = \frac{U_{max} + U_{min}}{2S_D R_{DC}} = \frac{7,3 + 1,7}{2 \cdot 0,3 \cdot 10000} = 1,5 \text{ mW}$  are calculated.

The sensitivity of the homodyne vibrometer in the bandwidth 30 kHz to 1 GHz is

$$S = R_{AC} \cdot S_D \cdot \frac{4\pi}{\lambda} P_0 \cdot m = 700 \cdot 0,3 \cdot \frac{4\pi}{532 \cdot 10^{-9}} \cdot 1,5 \cdot 10^{-3} \cdot 0,6221 \approx 4,63 \text{ mV/nm}$$

The quantum efficiency of the photodiode is:  $\eta = \frac{S_D \cdot hc}{e \cdot \lambda} = \frac{0,3 \cdot 6,62 \cdot 10^{-34} \cdot 3 \cdot 10^8}{1,6 \cdot 10^{-19} \cdot 532 \cdot 10^{-9}} = 0,7$

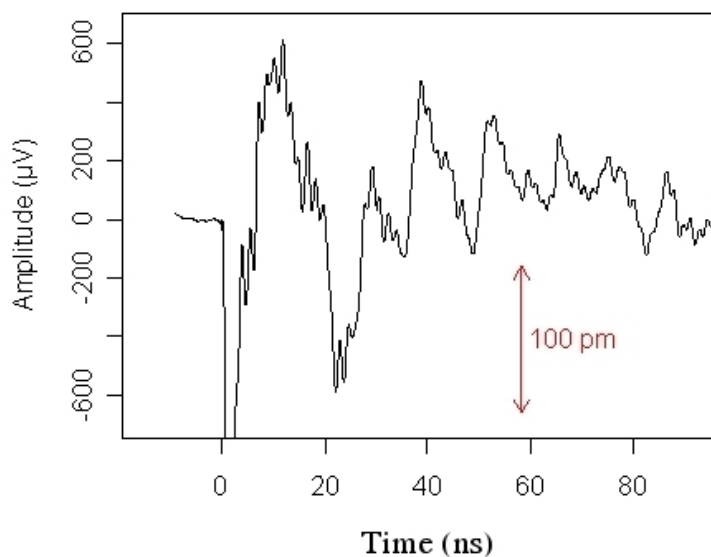
The noise equivalent displacement for a bandwidth of 1 GHz is:

$$\delta x = \frac{1}{2\pi m} \cdot \sqrt{\frac{hc \lambda \cdot \Delta f}{2\eta P_0}} = \frac{1}{2\pi \cdot 0,622} \cdot \sqrt{\frac{6,62 \cdot 10^{-34} \cdot 3 \cdot 10^8 \cdot 532 \cdot 10^{-9} \cdot 10^9}{2 \cdot 0,7 \cdot 1,5 \cdot 10^{-3}}} = 57,4 \text{ pm} \approx 60 \text{ pm}$$

After the measurements that led to the determination of the sensitivity and of the NED, the homodyne interferometer is stabilized at its maximum sensitivity by looping the control system. The pump laser can be put into operation and vibrations are detected. In order to detect displacements smaller than  $0,1 \text{ pm}$ , the signal-to-noise ratio should be multiplied by 600, by working out the average of at least  $600^2 = 360000$  signals. In theory, at a repetition rate of 10 kHz for the pump laser, it will take 36 s. In practice, the calculating time must be added. It depends on the number of points set for the signal acquisition.

The acquisitions were made with a numerical oscilloscope which can sample at a frequency of 20 GigaSamples/s. The total length of an acquisition is 500 ns, which corresponds to a data volume of 10,000 points per acquisition. The average of  $10^6$  acquisitions is shown on figure 1 during the first 100 nanoseconds.

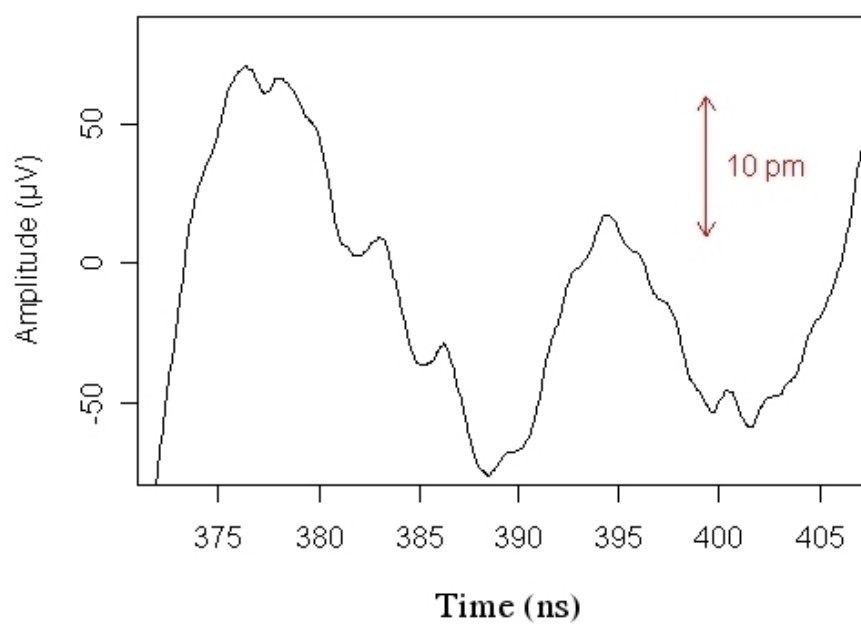
## Ultrasonic signal of a gold film on silicon



The vertical resolution is of 8 bits for a single acquisition, and of 16 bits for the averaged signal. The signal digitised on 16 bits and having an amplitude of about 2 mV corresponds to a quantum of digitisation equal to  $2 \text{ mV} / 2^{16} \approx 30 \text{ nV}$ .

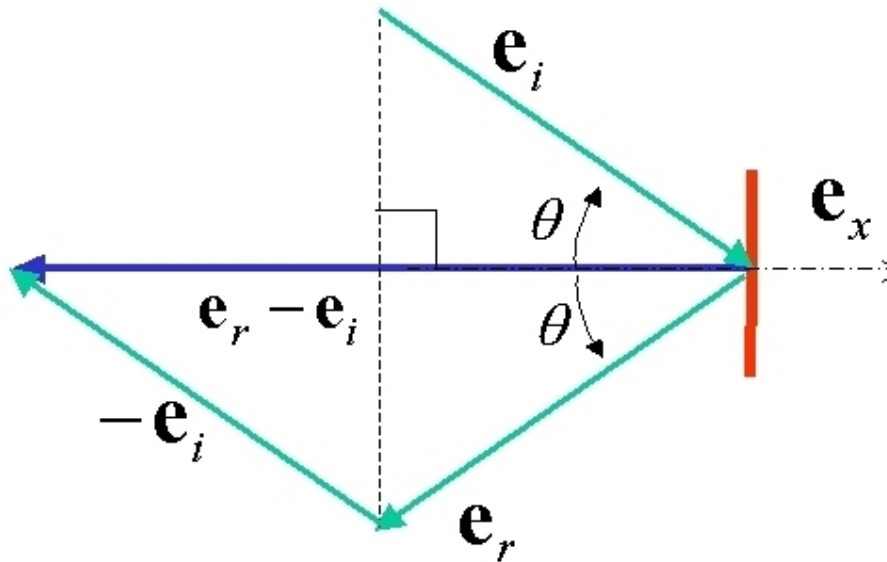
The noise equivalent displacement on the averaged signal is  $60 \text{ pm} / \sqrt{(10^{-6})} = 60 \text{ fm}$ . The RMS value of the noise in the signal is approximately equal to  $60 \text{ fm} \cdot 5 \text{ mV/nm} = 0,3 \text{ } \mu\text{V}$ , that is a value 10 times greater than the quantum of digitisation. This calculation shows that the main limiting factor is the noise of the signal. By increasing the averaged signal (figure 2), it is demonstrated that the RMS value of the noise is approximately equal to the calculated value. Thanks to the SNR, displacements of 100 fm can be measured.

## Ultrasonic signal of a gold film on silicon



# III.Exercises

## 1. Questions



### Question 1

[Solution n°1 p 44]

On the illustration, calculate the expression of the interference signal from the homodyne Mach-Zehnder interferometer, according to the position  $x$  of the target.

### Question 2

[Solution n°2 p 44]

A vibrometer is constructed on a homodyne two-beam interferometer, stabilised at its maximum sensitivity. Calculate the **sensitivity** of the vibrometer at the current outlet of the photodetector, in  $\mu\text{A}/\text{nm}$ . The parameters of the interferometer and of the photodetector are: incident power on the photodetector  $P_0 = 0.1 \text{ mW}$ , efficiency of the photodetector  $\eta = 0.8$ , wavelength of the probe beam  $\lambda = 633 \text{ nm}$ , interference contrast  $m = 0.5$ .

### Question 3

[Solution n°3 p 44]

A vibrometer is constructed on a homodyne two-beam interferometer, stabilized at its maximum sensitivity. Calculate the **noise equivalent displacement** of the vibrometer at the current outlet of the photodetector, with a bandwidth of  $1 \text{ MHz}$ . The parameters of the interferometer and of the photodetector are: incident power on the photodetector  $P_0 = 0.1 \text{ mW}$ , efficiency of the photodetector  $\eta = 0.8$ , wavelength of the probe beam  $\lambda = 633 \text{ nm}$ , interference contrast  $m = 0.5$ .

### Question 4

[Solution n°4 p 44]

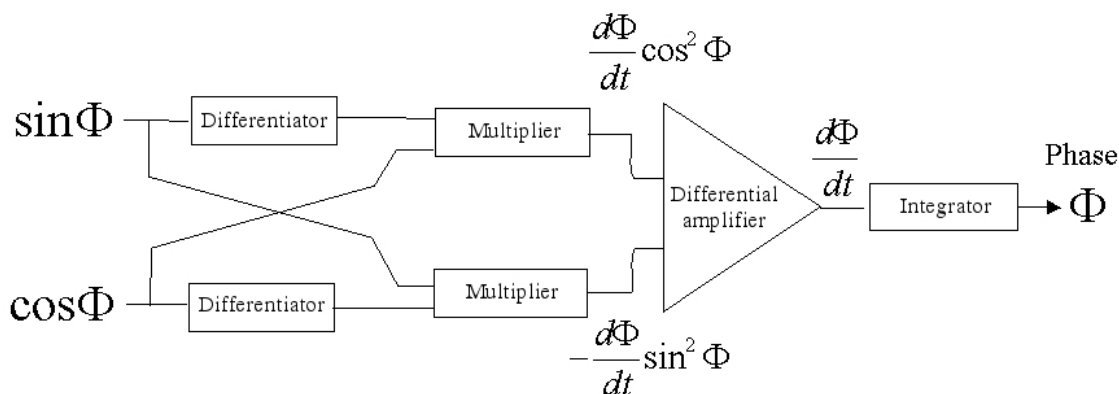
A homodyne two-beam interferometer is characterised by a noise equivalent displacement of  $\delta x = 10 \text{ fm.HZ}^{-1/2}$ . What is the minimum number of acquisitions to be averaged in order to detect sinusoidal vibrations with an amplitude of  $0.1 \text{ pm}$ , at a frequency of  $100 \text{ MHz}$ ?

## 2. Exercise

A homodyne interferometer issues four signals in quadrature,  $I_1 = I_0(1 + m\sin\phi)$ ,  $I_2 = I_0(1 - m\sin\phi)$ ,  $I_3 = I_0(1 - m\cos\phi)$  and  $I_4 = I_0(1 + m\cos\phi)$  in which  $\phi = 4\pi x/\lambda + \phi_0$  is the phase. These four signals will allow you to extract the phase's cosine and sine  $\cos\phi$  and  $\sin\phi$  depending on the time  $t$ . We simulate the displacement of a target using a periodic movement:

$$x(t) = A\cos\omega t + \frac{A}{3}\cos 3\omega t + \frac{A}{5}\cos 5\omega t \quad \text{with } A = 8\lambda.$$

The displacement signal is represented by the figure.



### Question

[Solution n°5 p 44]

1. copy and paste the text written on the program below: « *GenSignalHomodyne.R* » on the Notepad or any other text editor, then save it as « *GenSignalHomodyne.R* », with a ".R" extension. Run the R program (see reference below) which will generate 10,000  $\cos\phi$  and  $\sin\phi$  points over the signal period. Results will be saved on a text file « *Homodyne\_CosSin.txt* », structured as indicated: the first column represents the time, the second one the phase's cosine and the third one its sine.

The program « *GenSignalHomodyne.R* » is written in the R language and environment. This is an open-source software. To run the program, you need to download the software setup program at: [www://R-project.org](http://www.R-project.org)<sup>2</sup>.

To get information about the R environment, you can find a PDF document entitled "R for rookies" at [http://cran.r-project.org/doc/contrib/Paradis-rdebuts\\_fr.pdf](http://cran.r-project.org/doc/contrib/Paradis-rdebuts_fr.pdf). {Référence }R: A language and environment for statistical computing. R Foundation for Statistical Computing, Vienna, Austria. ISBN 3-900051-07-0, URL <http://www.R-project.org><sup>3</sup>.

The following program « *GenSignalHomodyne.R* » can generate a database : | time |  $\cos\phi$  |  $\sin\phi$  |.

**Link to the document:** (cf. *GenSignalHomodyne.R.pdf*)

2. Create a program (using the R language or any other one) which will load the data saved in the text file « *Homodyne\_CosSin.txt* » then make a **numerical phase demodulation**  $\phi$  in order to find the displacement

$$x(t) = A\cos\omega t + \frac{A}{3}\cos 3\omega t + \frac{A}{5}\cos 5\omega t$$

2 - [www://R-project.org](http://www.R-project.org)

3 - <http://www.R-project.org>

# Solution des exercices

## >Solution n°1 (exercice p. 42)

Let's calculate the instantaneous Doppler shift  $\delta\nu_D(t) = \frac{\vec{v}(t) \cdot (\vec{e}_r - \vec{e}_i)}{\lambda} = \frac{-2\cos\theta \times v_x(t)}{\lambda}$ . The interference signal is  $I = I_0(1 + m \cos \Phi)$  with  $\phi = \frac{-4\pi \cos\theta \times x(t)}{\lambda} + \Phi_0$ . The sensitivity decreases with the angle  $\theta$ .

## >Solution n°2 (exercice p. 42)

The sensitivity is  $S = S_D \cdot \frac{4\pi}{\lambda} P_0 \cdot m$  with the following sensitivity for the photodetector:

$$S_D = n \cdot \frac{e\lambda}{hc} = 0,8 \cdot \frac{1,6 \cdot 10^{-19} \cdot 633 \cdot 10^{-9}}{6,62 \cdot 10^{-34} \cdot 3 \cdot 10^8} = 0,41 \text{ A/W}$$

Hence:

$$S = S_D \cdot \frac{4\pi}{\lambda} P_0 \cdot m = 0,41 \cdot \frac{4\pi}{633 \cdot 10^{-9}} \cdot 0,1 \cdot 10^{-3} \cdot 0,5 \approx 405 \text{ A/m} \approx 0,40 \mu \text{ A/nm}$$

## >Solution n°3 (exercice p. 42)

The noise equivalent displacement expression is:

$$\delta x = \frac{1}{2\pi m} \cdot \sqrt{\frac{hc \cdot \lambda f}{2_n P_0}} = \frac{1}{2\pi \cdot 0,5} \cdot \sqrt{\frac{6,62 \cdot 10^{-34} \cdot 3 \cdot 10^8 \cdot 633 \cdot 10^{-9} \cdot 10^6}{2 \cdot 0,8 \cdot 0,1 \cdot 10^{-3}}} \approx 9 \text{ pm}$$

## >Solution n°4 (exercice p. 42)

The noise equivalent displacement expression is:  $\delta x' = \delta x_S \cdot \sqrt{\frac{\Delta f}{N}}$ ,  $\delta x' = 10 \text{ pm} / \sqrt{\text{Hz}}$ ,  $N$  is the number of acquisitions and  $\Delta f$  is the bandwidth.

Hence:

$$N = \Delta f \cdot \left(\frac{\delta x_0}{\delta x}\right)^2 = 10^8 \cdot \left(\frac{10 \cdot 10^{-15}}{0,1 \cdot 10^{-12}}\right)^2 = 10^6$$

## >Solution n°5 (exercice p. 43)

The following program « EXERCICE\_Démodule\_Homodyne.R » written in R language, numerically demodulates fringes. It relies on the diagram shown in figure 18 « Principle of the analogue demodulation of two signals in quadrature ».

Comment : it is possible to directly extract the phase  $\phi$  modulo  $2\pi$ . When it is done, create a phase sequencing algorithm to find the displacement  $x(t)$

**Link to the document:** (cf. GenSignalHomodyne.R(solution).pdf)

# Bibliographie

[[1]] SCRUBY C.B., DRAIN L.E., *Laser Ultrasonics*, Adam Hilger, Bristol, Philadelphia and New York, 1990.

[[2]] DEWHURST R.J., SHAN Q., *Optical Remote measurement of Ultrasound*, Meas. Sci. Technol., 1999, 10, R139.

[[3]] ROYER DANIEL, *Génération et détection optiques d'ondes élastiques*, Techniques de l'ingénieur, E4415.

# Webographie

[[4]] <http://www.faro.com> (consultation 29 06 2007).

[[5]] <http://www.polytec-pi.fr/> (consultation 29 06 2007).